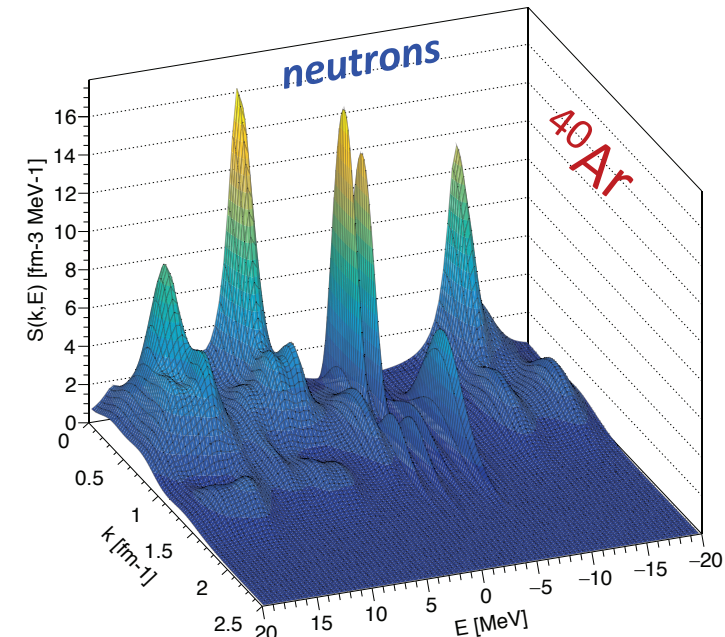
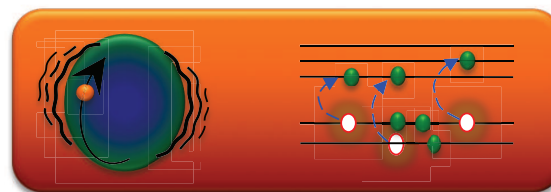
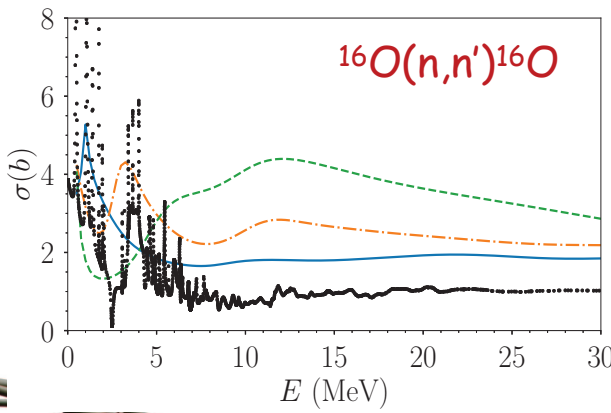
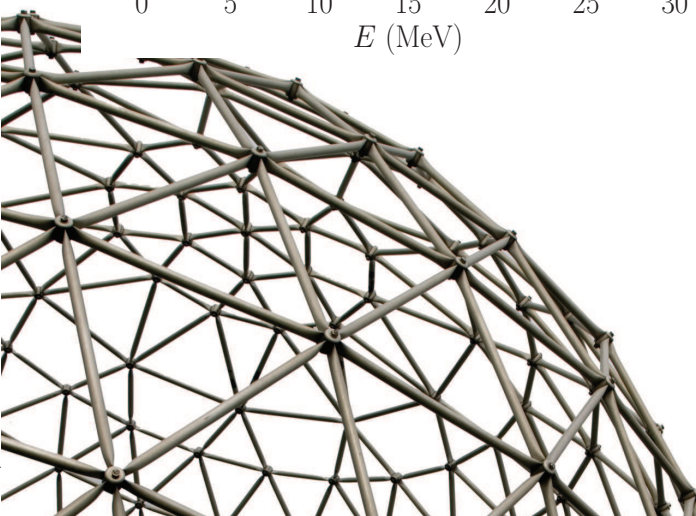


Recent *ab initio* studies of nuclei from self-consistent Green's functions theory

Carlo Barbieri — University of Surrey

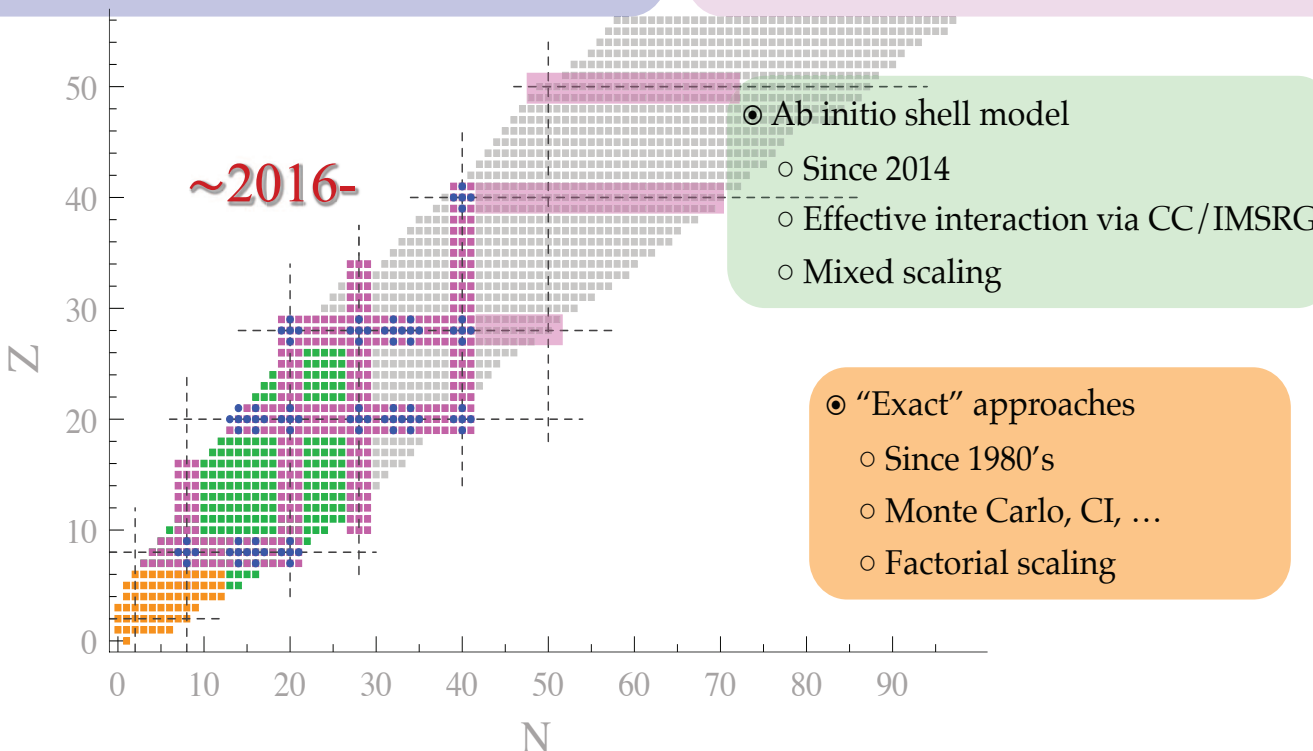
11 December 2019



Reach of ab initio methods across the nuclear chart

- Approximate approaches for closed-shell nuclei
 - Since 2000's
 - SCGF, CC, IMSRG
 - Polynomial scaling

- Approximate approaches for open-shells
 - Since 2010's
 - GGF, BCC, MR-IMSRG
 - Polynomial scaling



Key developments for (nuclear) SCGF:

Dyson ADC(2), ADC(3)

Schirmer 1982

Dyson ADC(4), ADC(5)

Schirmer 1983 (formalism)

Particle-vibration coupling, FRPA(3)

CB 2000, 2007

Gorkov ADC(2): open shells!

Somà 2011, 2013

3-nucleon forces basic formalism

Carbone, Cipollone 2013

3NFs in Dyson ADC(3)

Raimondi 2018

Gorkov ADC(3) and higher orders (automatic)

Raimondi, Arthus 2019

Deformation – still needed...

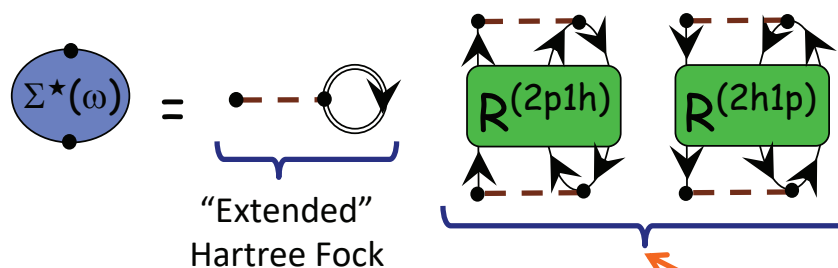
???

Symmetry restoration – still needed...

???

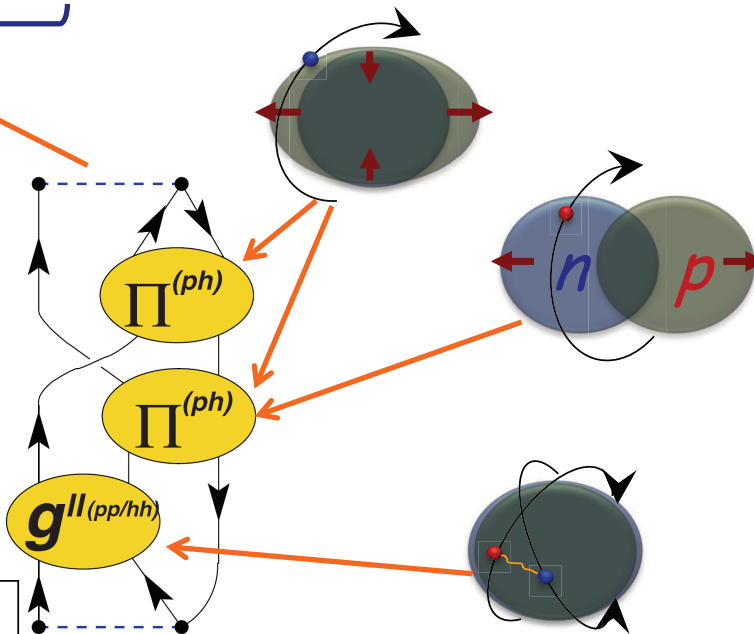
The FRPA Method in Two Words

Particle vibration coupling is the main mechanism driving the redistribution and fragmentation of particle strength—especially in the quasielastic regions around the Fermi surface...

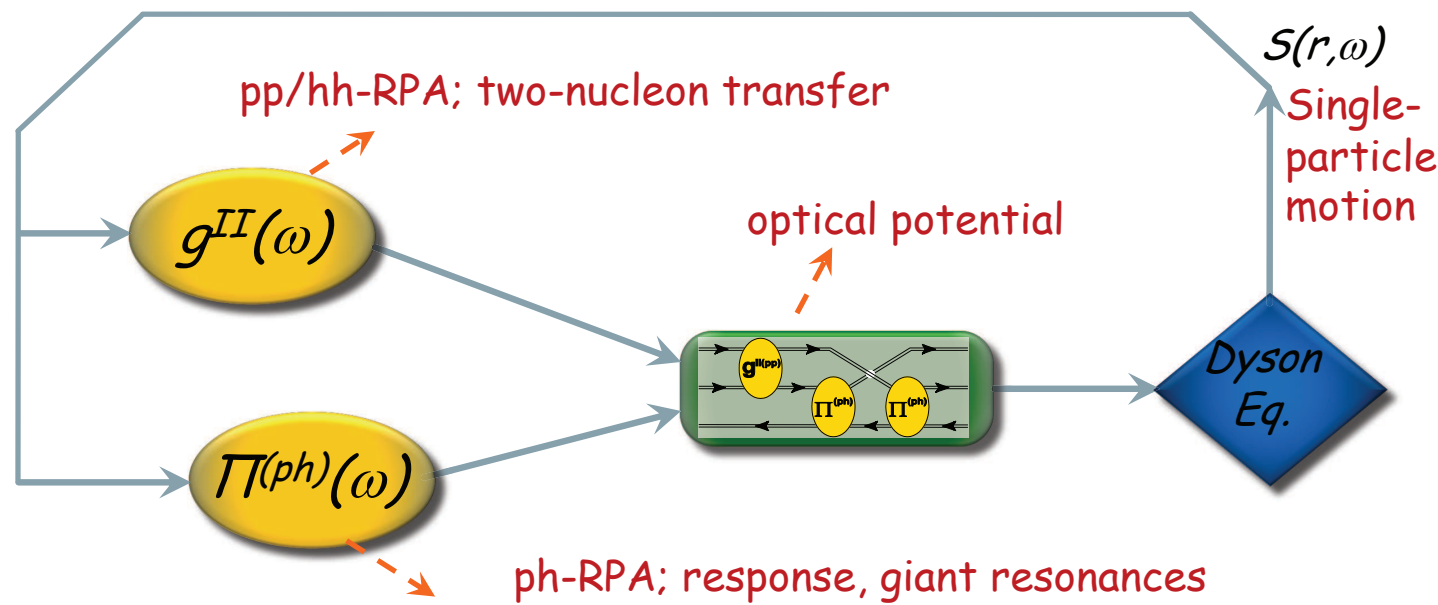


CB et al.,
Phys. Rev. C63, 034313 (2001)
Phys. Rev. A76, 052503 (2007)
Phys. Rev. C79, 064313 (2009)

- A complete expansion requires all types of particle-vibration coupling
 - ...these modes are all resummed exactly and to all orders in a *ab initio* many-body expansion.
- The Self-energy $\Sigma^*(\omega)$ yields both single-particle states and scattering

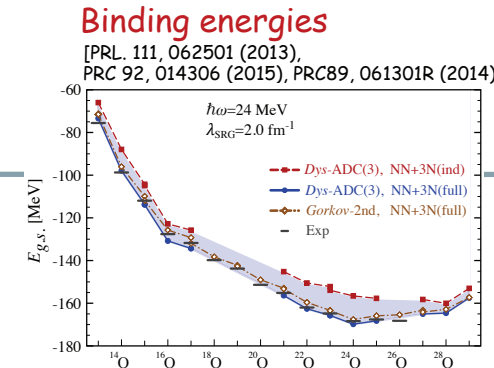
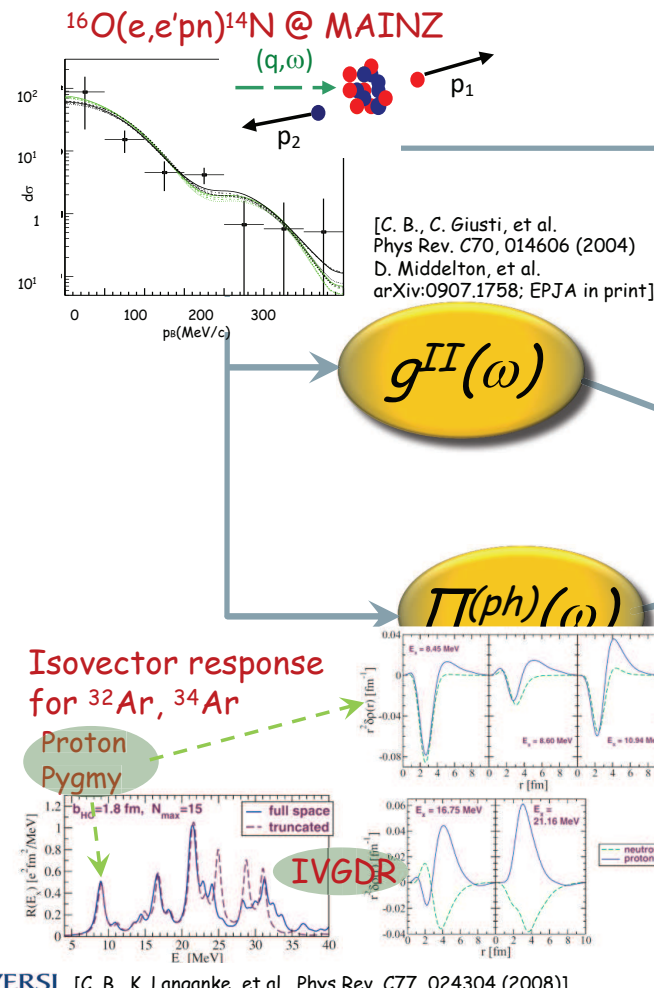


Self-Consistent Green's Function Approach



- Global picture of nuclear dynamics
- Reciprocal correlations among effective modes
- Guarantees *macroscopic conservation laws*

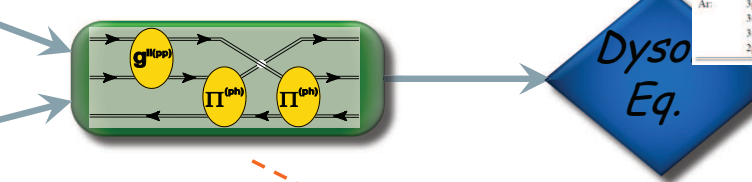
Self-Consistent Green's Function Approach



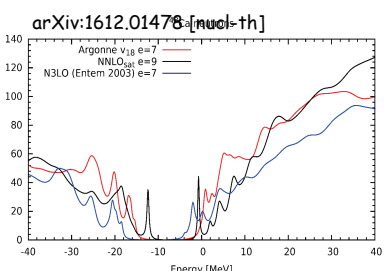
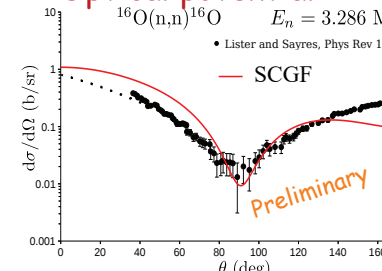
Ionization energies/
affinities, in atoms

[C.B., D. Van Neck,
AIP Conf. Proc. 1120, 104 ('09) & in prep]

	Hartree-Fock	FRPAc	Experiment [16, 17]
He:	1s	0.918 (+14)	0.9008 (-2.9)
Be ²⁺ :	1s	5.6672 (+116)	5.6551 (-0.5)
Be:	2s	0.3093 (-34)	0.3224 (-20.2)
	1s	4.733 (+200)	4.5405 (+8)
Ne:	2p	0.852 (+57)	0.8037 (+11)
	1s	1.931 (+149)	1.7967 (+15)
Mg ²⁺ :	2p	3.0068 (+56.9)	2.9537 (+3.8)
	1s	4.4827	4.3589
Mg:	3s	0.253 (-28)	0.280 (-1)
	2p	2.282 (-162)	2.137 (+17)
Ar:	3p	0.591 (+12)	0.579 (=0)
	3s	1.277 (+202)	1.065 (-10)
	3s		1.544
	2p	9.571 (+411)	9.219 (+59)
			9.160

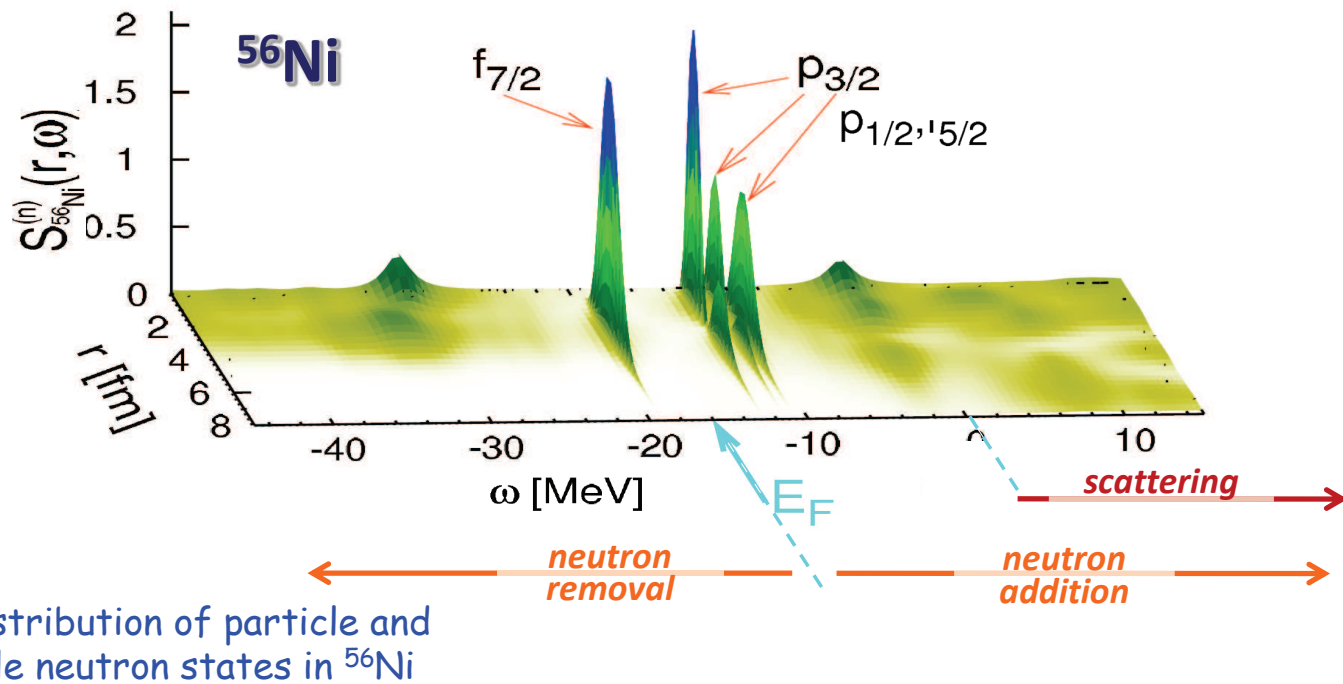


Optical potential



One-nucleon spectral function

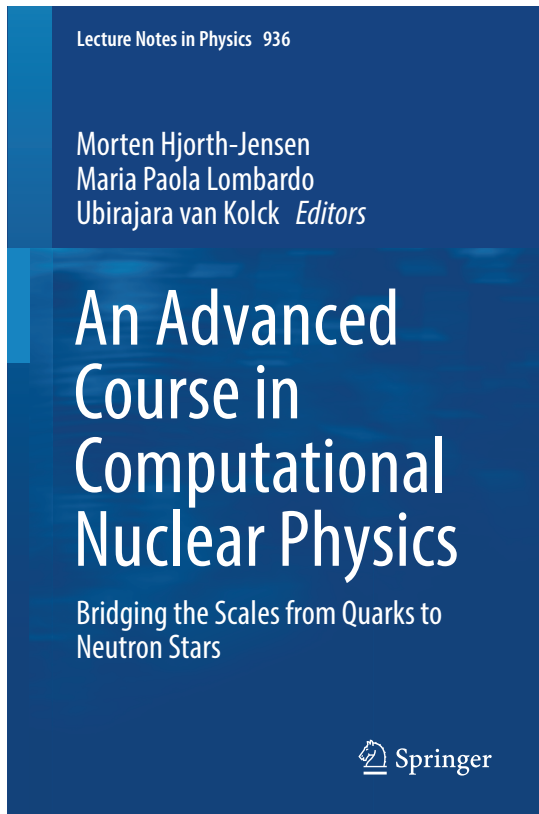
$$S^{p,h}(r, \omega) = \mp \frac{1}{\pi} \operatorname{Im} g(r = r'; \omega)$$



W. Dickhoff, CB, Prog. Part. Nucl. Phys. 53, 377 (2004)
CB, M.Hjorth-Jensen, Phys. Rev. C79, 064313 (2009)

Ab-initio Nuclear Computation & BcDor code

Self-consistent Green's function formalism
and methods for Nuclear Physics



CB and A. Carbone,
chapter 11 of
Lecture Notes in Physics 936 (2017)

Lecture Notes in Physics 936

Morten Hjorth-Jensen
Maria Paola Lombardo
Ubirajara van Kolck *Editors*

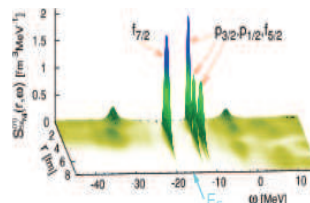
An Advanced Course in Computational Nuclear Physics

Bridging the Scales from Quarks to Neutron Stars

Springer

<http://personal.ph.surrey.ac.uk/~cb0023/bcdor/>

Computational Many-Body Physics



Download

Documentation

Welcome

From here you can download a public version of my self-consistent Green's function (SCGF) code for nuclear physics. This is a code in J-coupled scheme that allows the calculation of the single particle propagators (a.k.a. one-body Green's functions) and other many-body properties of spherical nuclei.

This version allows to:

- Perform Hartree-Fock calculations.
- Calculate the correlation energy at second order in perturbation theory (MBPT2).
- Solve the Dyson equation for propagators (self consistently) up to second order in the self-energy.
- Solve coupled cluster CCD (doubles only!) equations.

When using this code you are kindly invited to follow the creative commons license agreement, as detailed at the weblinks below. In particular, we kindly ask you to refer to the publications that led the development of this software.

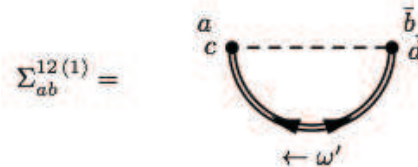
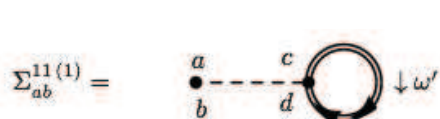
Relevant references (which can also help in using this code) are:

- Prog. Part. Nucl. Phys. 52, p. 377 (2004),
Phys. Rev. A76, 052503 (2007),
Phys. Rev. C79, 064313 (2009),
Phys. Rev. C89, 024323 (2014)

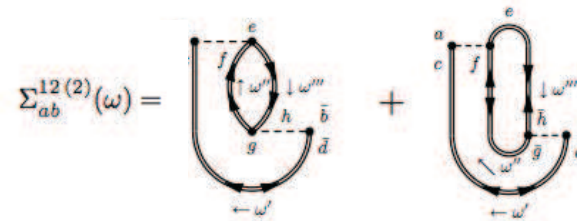
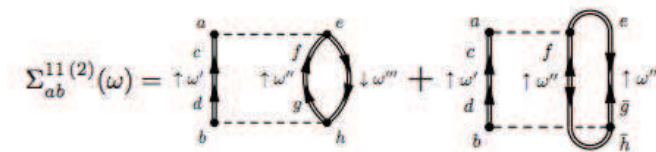
Open-shells: 1st & 2nd order Gorkov diagrams

V. Somà, CB, T. Duguet, , Phys. Rev. C **89**, 024323 (2014)
 V. Somà, CB, T. Duguet, Phys. Rev. C **87**, 011303R (2013)
 V. Somà, T. Duguet, CB, Phys. Rev. C **84**, 064317 (2011)

✳ 1st order → energy-independent self-energy



✳ 2nd order → energy-dependent self-energy



✳ Gorkov equations → eigenvalue problem

$$\sum_b \begin{pmatrix} t_{ab} - \mu_{ab} + \Sigma_{ab}^{11}(\omega) & \Sigma_{ab}^{12}(\omega) \\ \Sigma_{ab}^{21}(\omega) & -t_{ab} + \mu_{ab} + \Sigma_{ab}^{22}(\omega) \end{pmatrix} \Big|_{\omega_k} \begin{pmatrix} U_b^k \\ V_b^k \end{pmatrix} = \omega_k \begin{pmatrix} U_a^k \\ V_a^k \end{pmatrix}$$

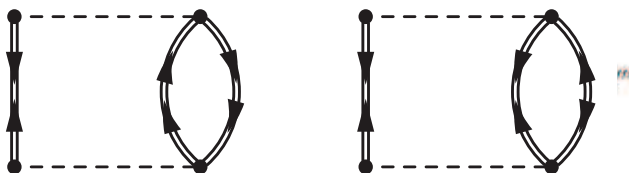
$$U_a^{k*} \equiv \langle \Psi_k | \bar{a}_a^\dagger | \Psi_0 \rangle$$

$$V_a^{k*} \equiv \langle \Psi_k | a_a | \Psi_0 \rangle$$

Reaching (Gorkov - 3NF - higher orders...) is a mess

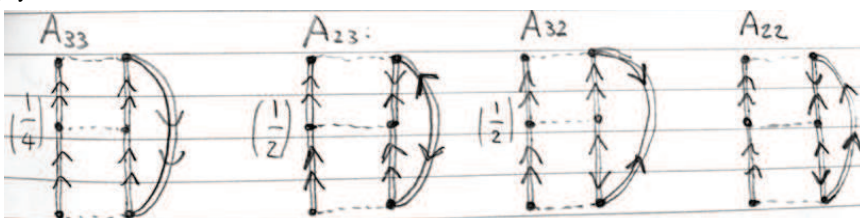
Gorkov at 2nd order and ONLY NN forces:

$$\Sigma_{ab}^{11(2)}(\omega) =$$

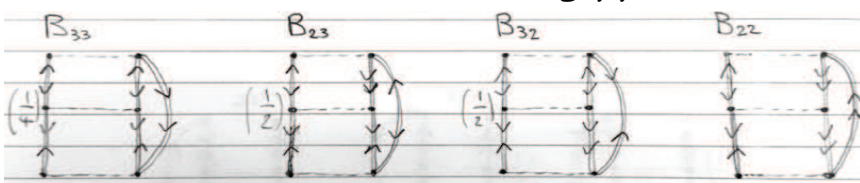


Gorkov at 3rd order and ONLY NN forces:

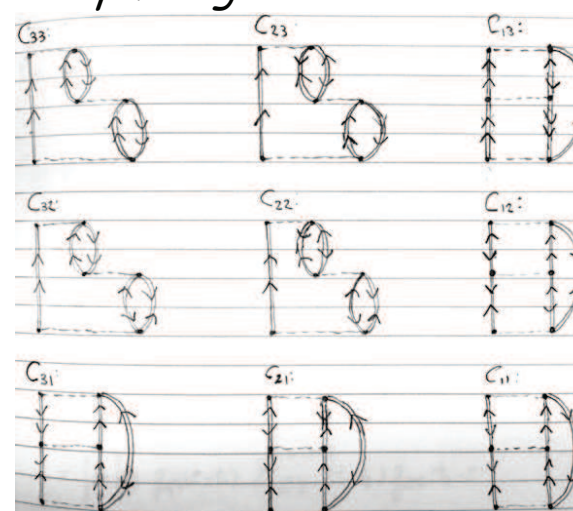
pp/hh-ladders:



hh-interactions (hh int. among pp ladders!!!)



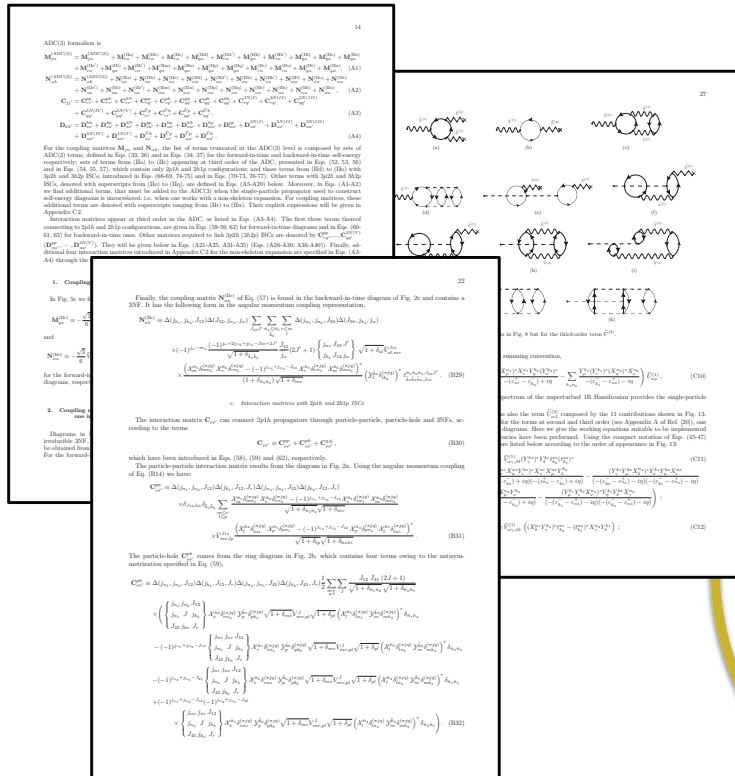
ph-rings:



Automatic generation of diagram needed
for 3NF and beyond...
→ F. Raimondi and P. Arthuis, in progress....

Inclusion of NNN forces

→ 3p2h/3h2p terms relevant to next-generation high-precision methods.



*Formalism already laid out:
F. Raimondi, CB, Phys. Rev. C97, 054308 (2018).*

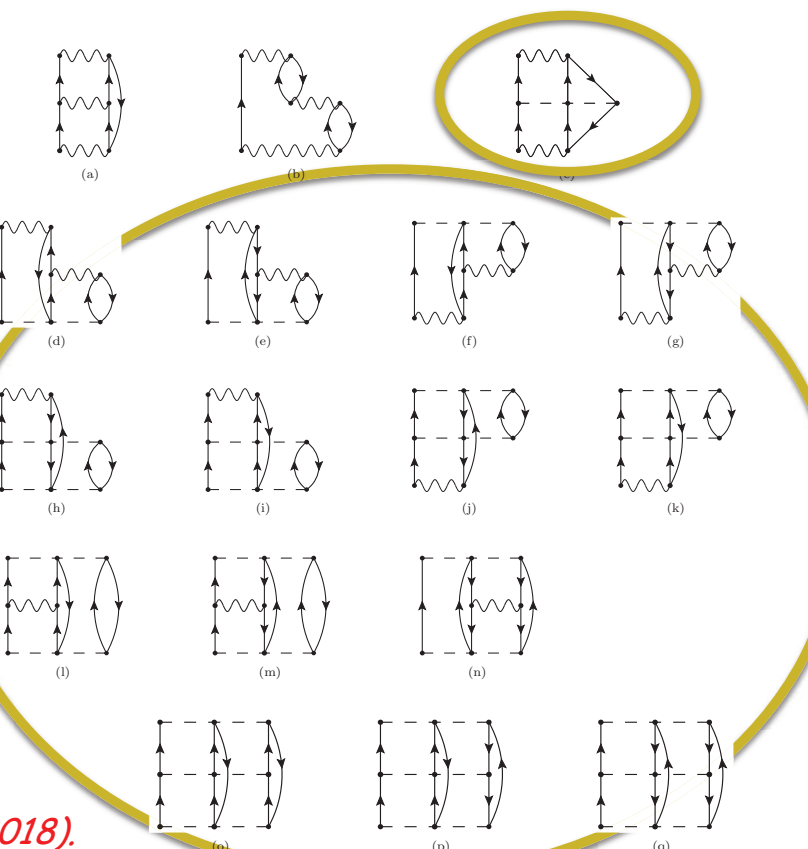


FIG. 5. 1PI, *skeleton* and *interaction irreducible* self-energy diagrams appearing at 3rd-order in perturbative expansion (7), making use of the effective hamiltonian of Eq. (9).

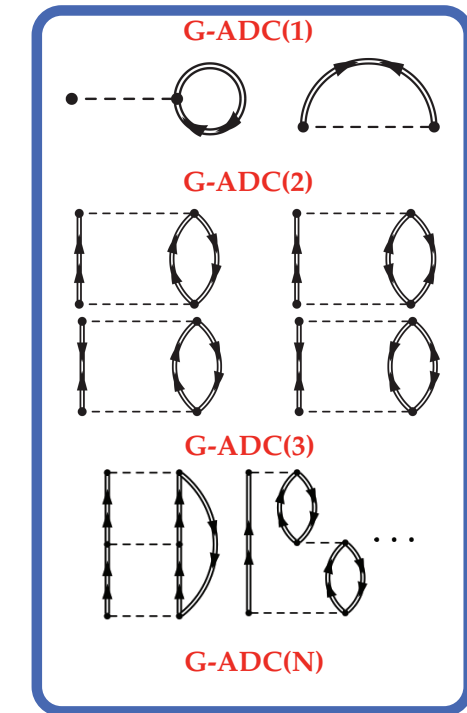
Automatic Diagrammatic Generation (ADG) of the self-energy

Goal: Drawing of self-energy Feynman diagrams and derivation of corresponding algebraic expressions are performed automatically

Background: ADG of the BMBPT expansion (P. Arthuis *et al* Comp. Phys. Comm. **240**, 202 (2019))

Feynman rules for Gorkov's self-energy
(V. Somà *et al* . Phys. Rev. C **84**, 064317 (2011))

- Symbolic computation (Python)
- Graph theory (NetworkX package)
- Formatting and drawing tools (LaTeX, TikZ package)



Features:

- Reach arbitrary order in the self-energy expansion
- Different treatments of the self-energy enabled:
perturbative/nonperturbative(ADC); Dyson/Gorkov; interaction reducible/irreducible, etc
- Faster and less error-prone than “human” derivation

Status:

- Drawing of the valid self-energy Feynman diagrams at arbitrary order completed
- Implementation of the rules to obtain algebraic expressions for the diagrams in progress

Work in progress by **F. Raimondi, CEA, Saclay**

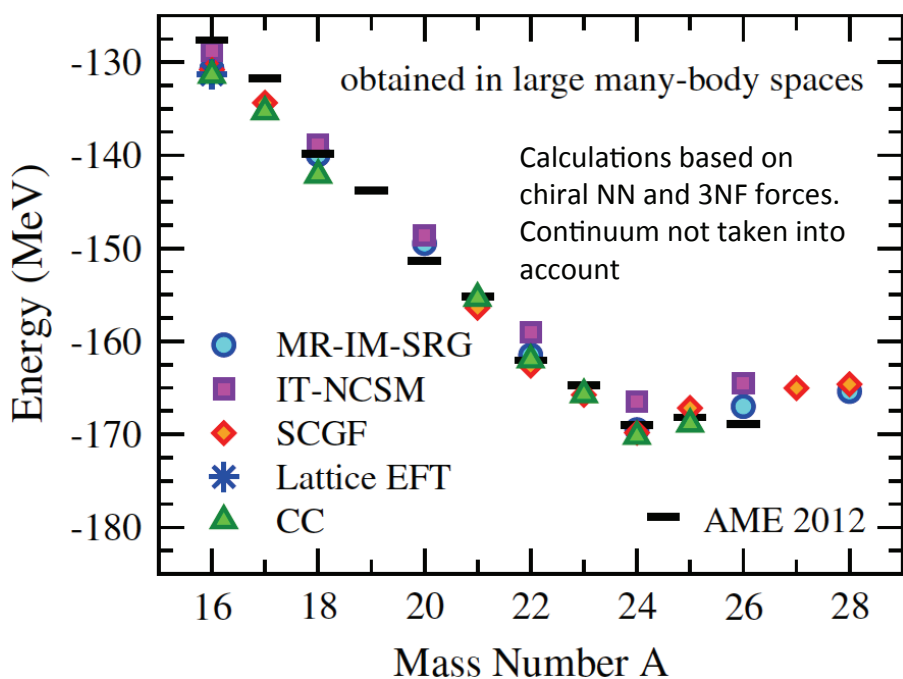
Chiral EFT interactions and 3-nucleon forces

in mid-mass isotopes

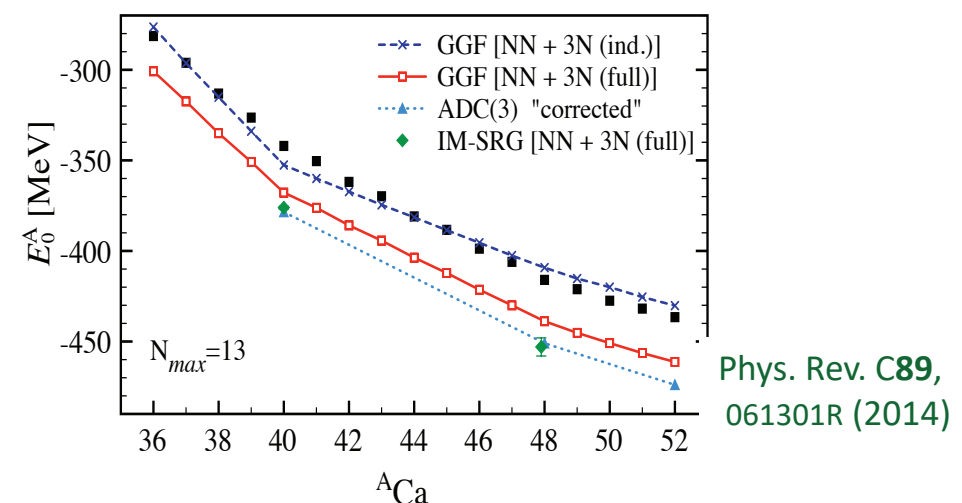
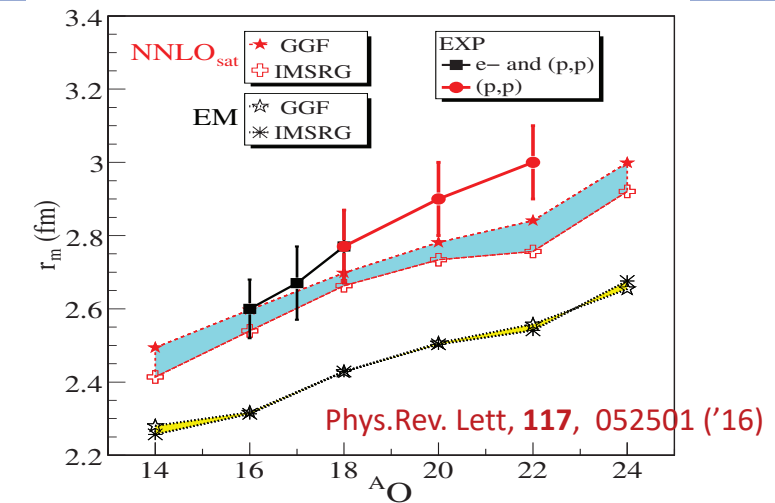
Benchmark of *ab-initio* methods for oxygen isotopic chain

First success of chiral-EFT interactions on oxygen isotopes....

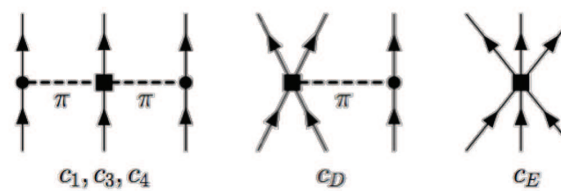
...but still poor for radii and larger isotopes:



Hebeler, Holt, Menendez, Schwenk, Ann. Rev. Nucl. Part. Sci. in press (2015)

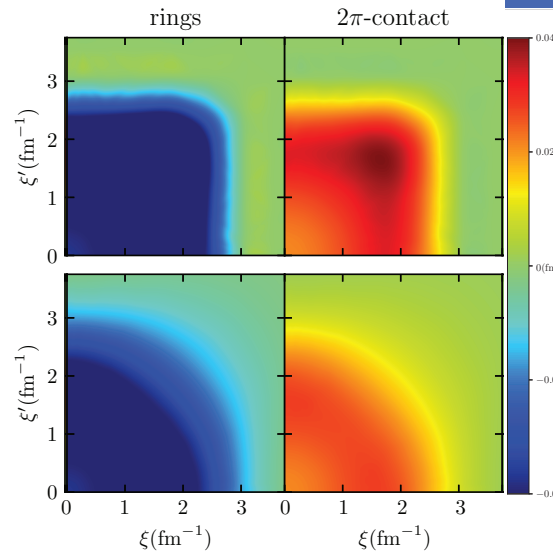


Local vs. non-local chiral N²LO NNN interaction – by P. Navrátil



nonlocal MS

local MS



- Local: chiral N³LO NN+ N²LO 3N500
 - $c_D = -0.2$ $c_E = -0.205$ (³H $E_{gs} = -8.48$ MeV)
- Non-local: chiral N²LO_{sat} NN+3N
 - $c_D = +0.8168$ $c_E = -0.0396$ (³H $E_{gs} = -8.53$ MeV)
- Local/Non-local: chiral N³LO NN+ N²LO
 - $c_D = +0.7$ $c_E = -0.06$ (³H $E_{gs} = -8.44$ MeV)

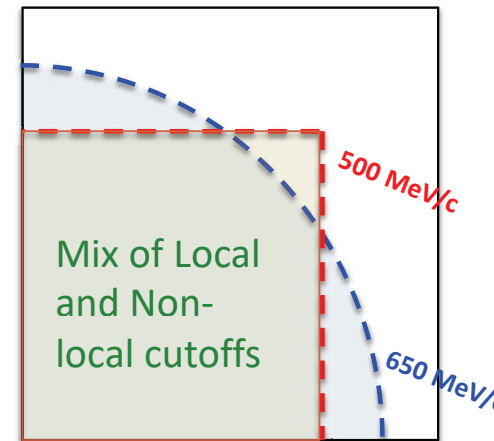
$$f_\Lambda^{\text{long}}(\mathbf{p}, \mathbf{q}) = \exp \left[-((\mathbf{p}^2 + 3/4 \mathbf{q}^2)/\Lambda^2)^n \right]$$

$$\langle \mathbf{p}' \mathbf{q}' | V_{3N}^{\text{reg}} | \mathbf{p} \mathbf{q} \rangle = f_R(\mathbf{p}', \mathbf{q}') \langle \mathbf{p}' \mathbf{q}' | V_{3N} | \mathbf{p} \mathbf{q} \rangle f_R(\mathbf{p}, \mathbf{q})$$

$$f_\Lambda^{\text{long}}(\mathbf{Q}_i) = \exp \left[-(Q_i^2/\Lambda^2)^2 \right]$$

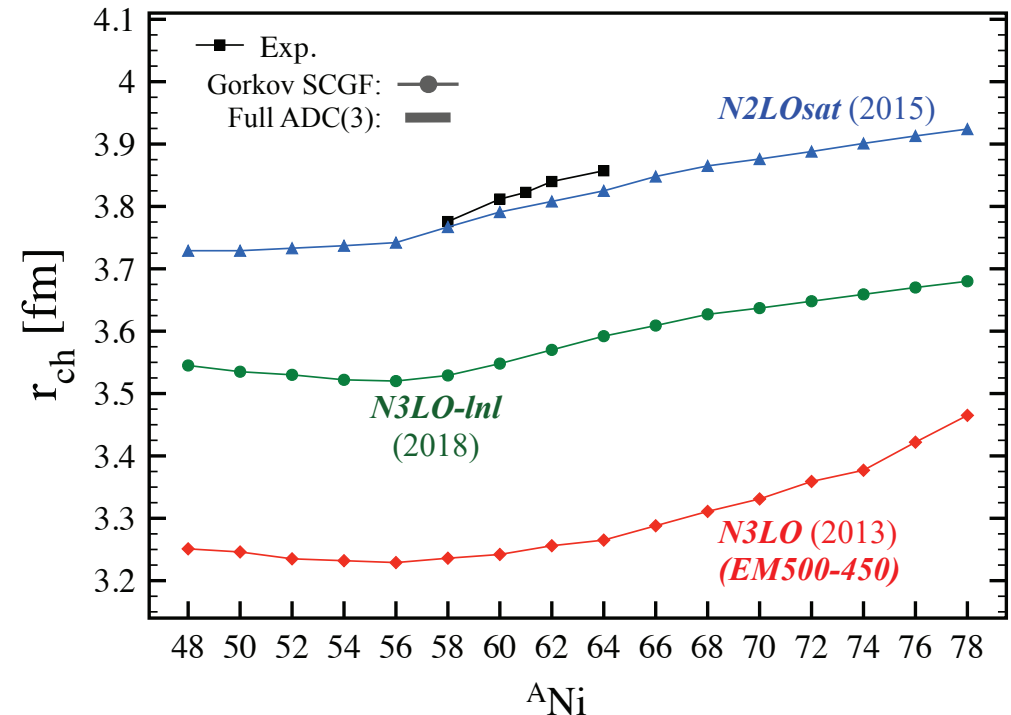
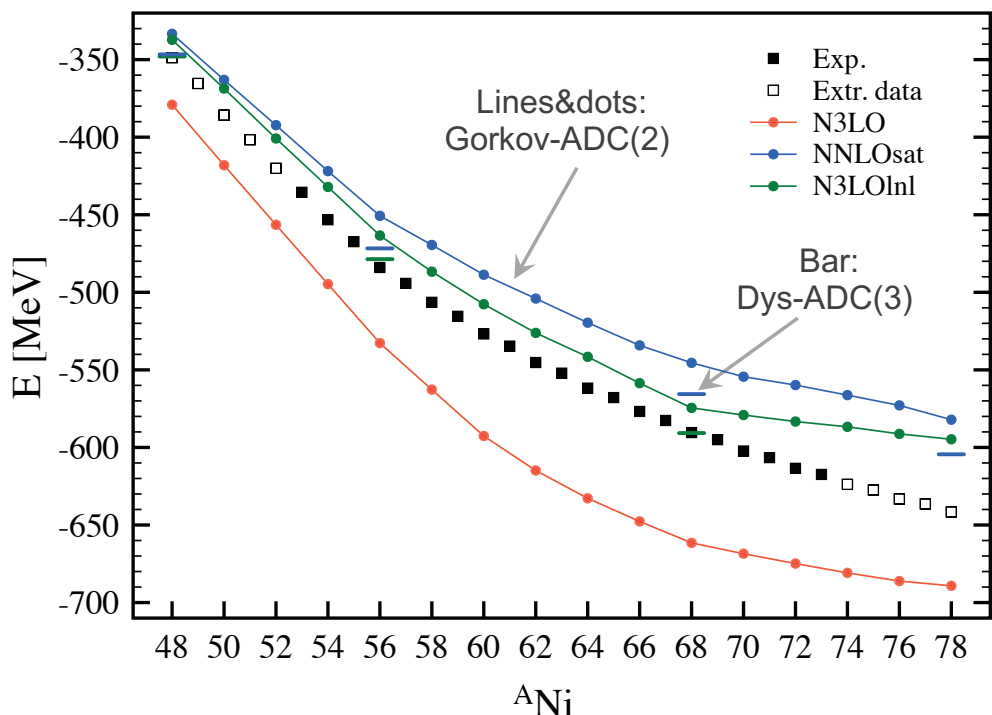
$$\langle \mathbf{p}' \mathbf{q}' | V_{3N}^{\text{reg}} | \mathbf{p} \mathbf{q} \rangle = \langle \mathbf{p}' \mathbf{q}' | V_{3N} | \mathbf{p} \mathbf{q} \rangle \prod_i f_R(\mathbf{Q}_i)$$

$\xi^2 = p^2 + 3/4 q^2 \approx 3\text{-nucleon tot. kinetic energy}$



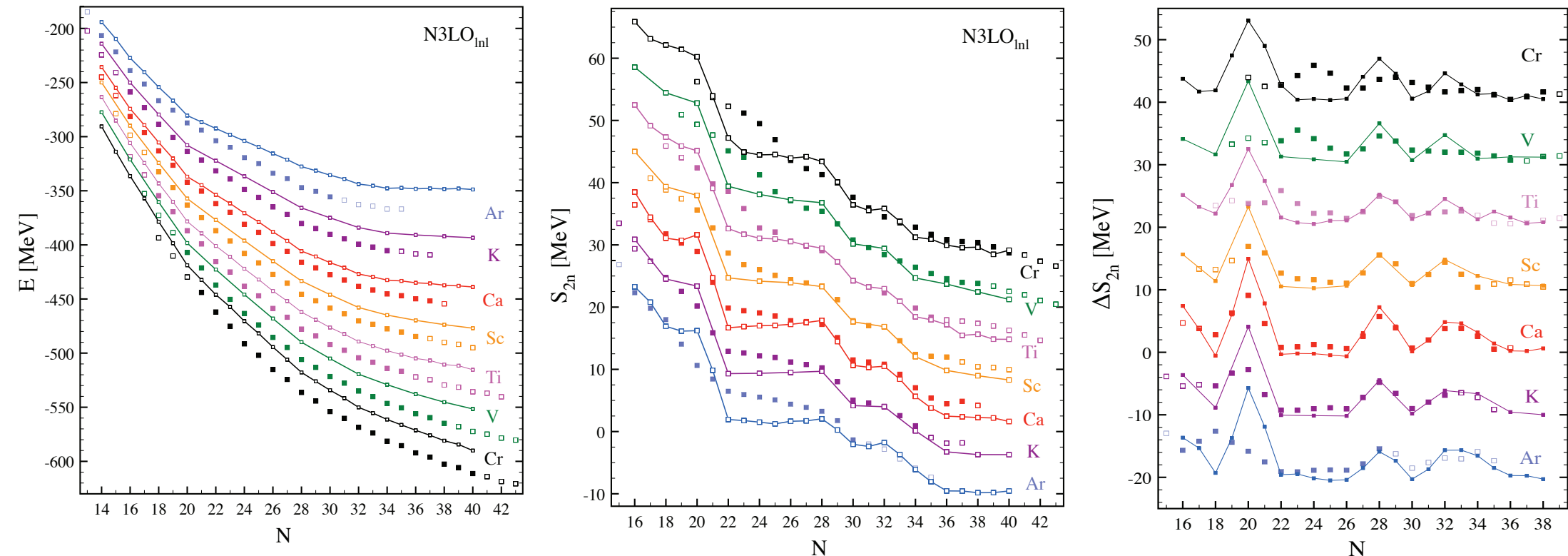
Plots courtesy of K. Hebeler (from his 7/1/19 talk)

Comparison of nuclear forces - ^ANi

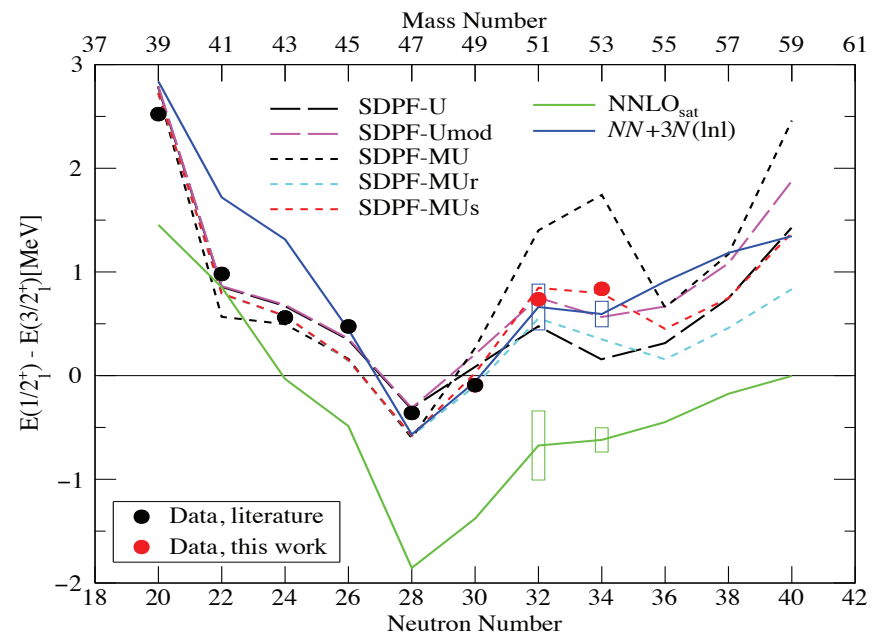
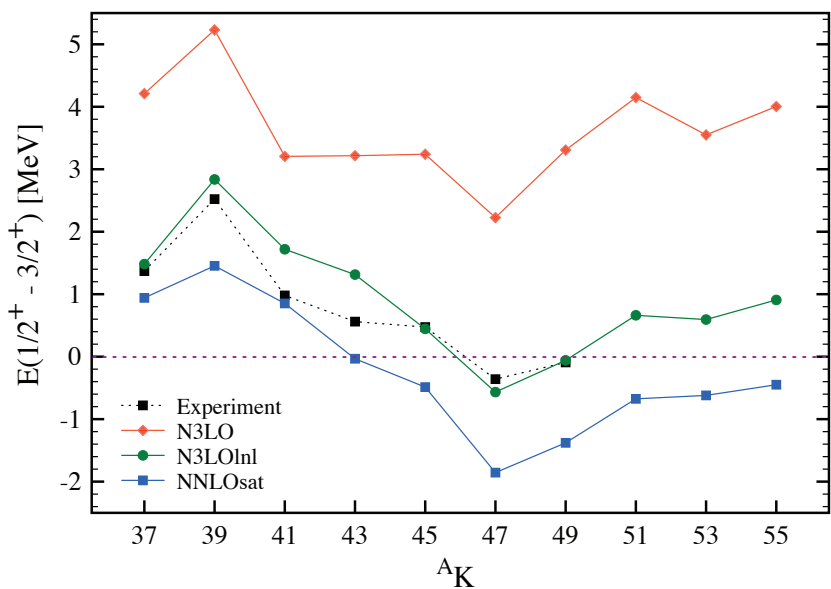


$N3LO(500) + n/n \ 3NF$

SCGF – Gorkov-ADC(2)



$d_{3/2} - s_{1/2}$ inversion in K isotopes



V. Somà, CB, et al., arXiv:1907:1907.09790

Papuga et al., PRL110, 172503 (2013); PRC90, 034321 (2014)

RIKEN, SEASTAR coll. (unpublished)

Ab initio optical potentials from propagator theory

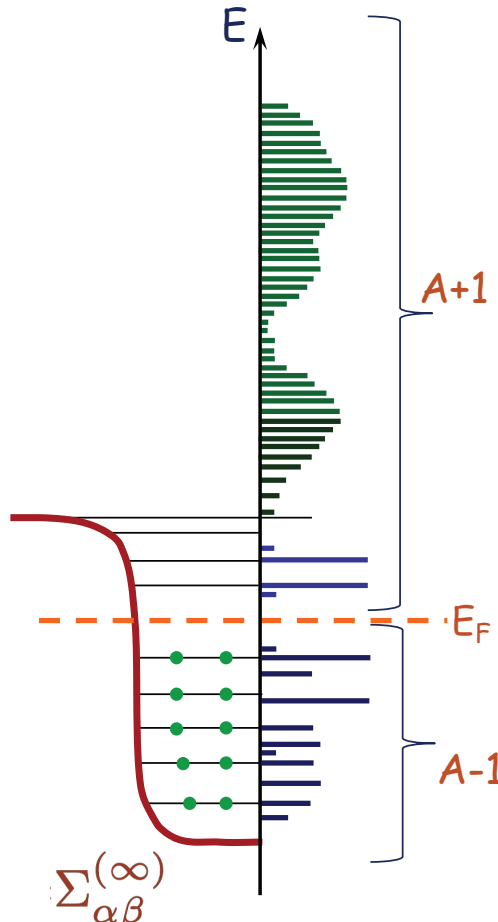
Relation to Fesbach theory:

Mahaux & Sartor, Adv. Nucl. Phys. 20 (1991)
Escher & Jennings Phys. Rev. C66, 034313 (2002)

Previous SCGF work:

CB, B. Jennings, Phys. Rev. C72, 014613 (2005)
S. Waldecker, CB, W. Dickhoff, Phys. Rev. C84, 034616 (2011)
A. Idini, CB, P. Navrátil, Phys. Rev. Lett. 123, 092501 (2019)

Microscopic optical potential



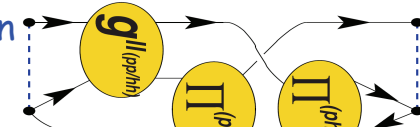
Nuclear self-energy $\Sigma^*(\mathbf{r}, \mathbf{r}'; \varepsilon)$:

- contains *both particle* and *hole* props.
- it is proven to be a Feshbach opt. pot \rightarrow in general it is *non-local* !

$$\Sigma_{\alpha\beta}^*(\omega) = \Sigma_{\alpha\beta}^{(\infty)} + \sum_{i,j} \mathbf{M}_{\alpha,i}^\dagger \left[\frac{1}{E - (\mathbf{K}^> + \mathbf{C}) + i\Gamma} \right]_{i,j} \mathbf{M}_{j,\beta}$$

$$+ \sum_{r,s} \mathbf{N}_{\alpha,r} \left[\frac{1}{E - (\mathbf{K}^< + \mathbf{D}) - i\Gamma} \right]_{r,s} \mathbf{N}_{s,\beta}^\dagger$$

mean-field
Particle-vibration
couplings:



Solve scattering and overlap functions directly in momentum space:

$$\Sigma^{*l,j}(k, k'; E) = \sum_{n, n'} R_{nl}(k) \Sigma_{n, n'}^{*l,j} R_{nl}(k')$$

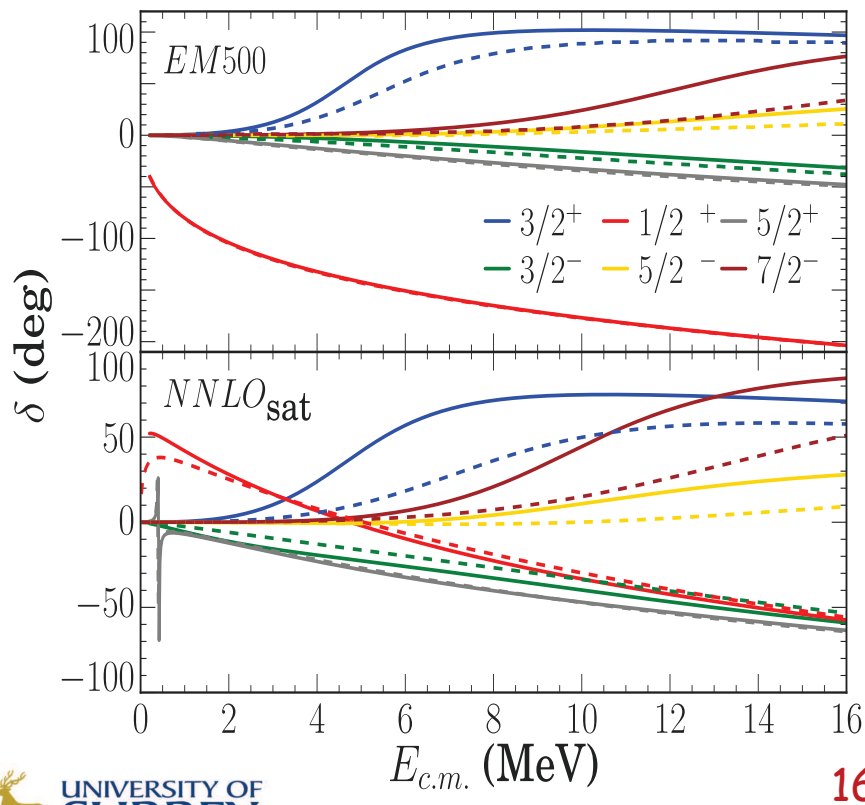
$$\frac{k^2}{2\mu} \psi_{l,j}(k) + \int dk' k'^2 \Sigma^{*l,j}(k, k'; E_{c.m.}) \psi_{l,j}(k') = E_{c.m.} \psi_{l,j}(k)$$

Low energy scattering - from SCGF

Benchmark with NCSM-based scattering.

[A. Idini, CB, Navratil,
Phys. Rev. Lett. **123**, 092501 (2019)]

Scattering from mean-field only:



— — — NCSM/RGM [without core excitations]

EM500: NN-SRG $\lambda_{SRG} = 2.66 \text{ fm}^{-1}$, Nmax=18 (IT)
[PRC **82**, 034609 (2010)]

NNLO_{sat}: Nmax=8 (IT-NCSM)

— — — SCGF [$\Sigma^{(\infty)}$ only], always Nmax=13



Low energy scattering - from SCGF

Benchmark with NCSM-based scattering.

[A. Idini, CB, Navratil,
Phys. Rev. Lett. **123**, 092501 (2019)]

Scattering from mean-field only:

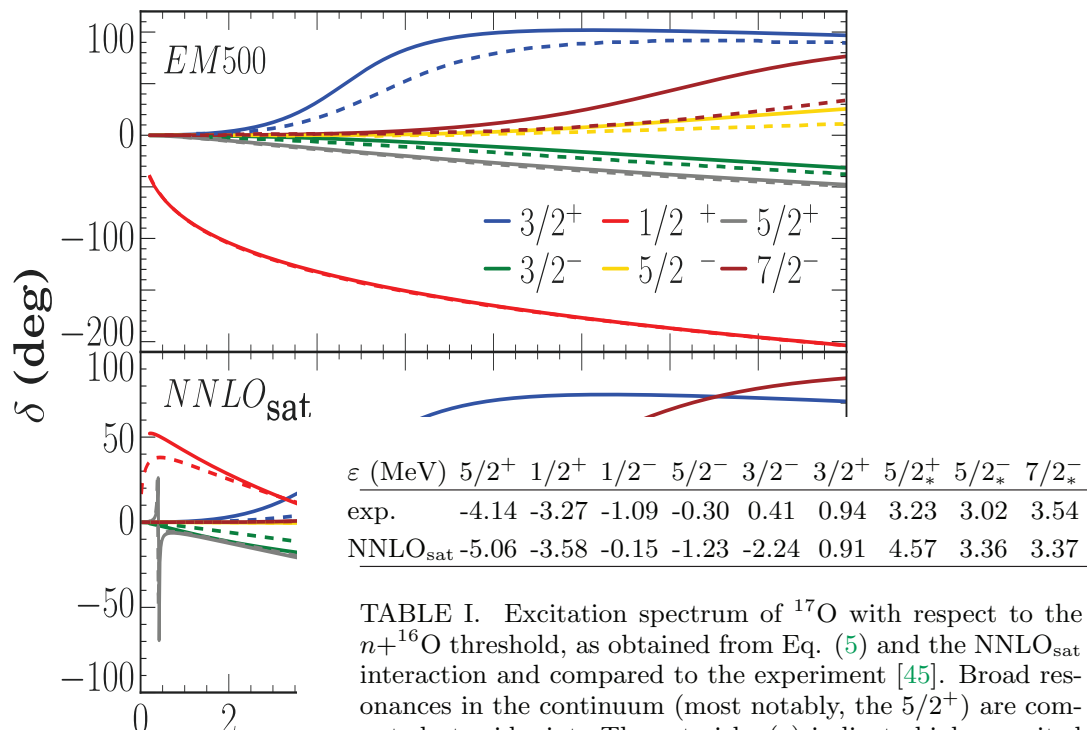
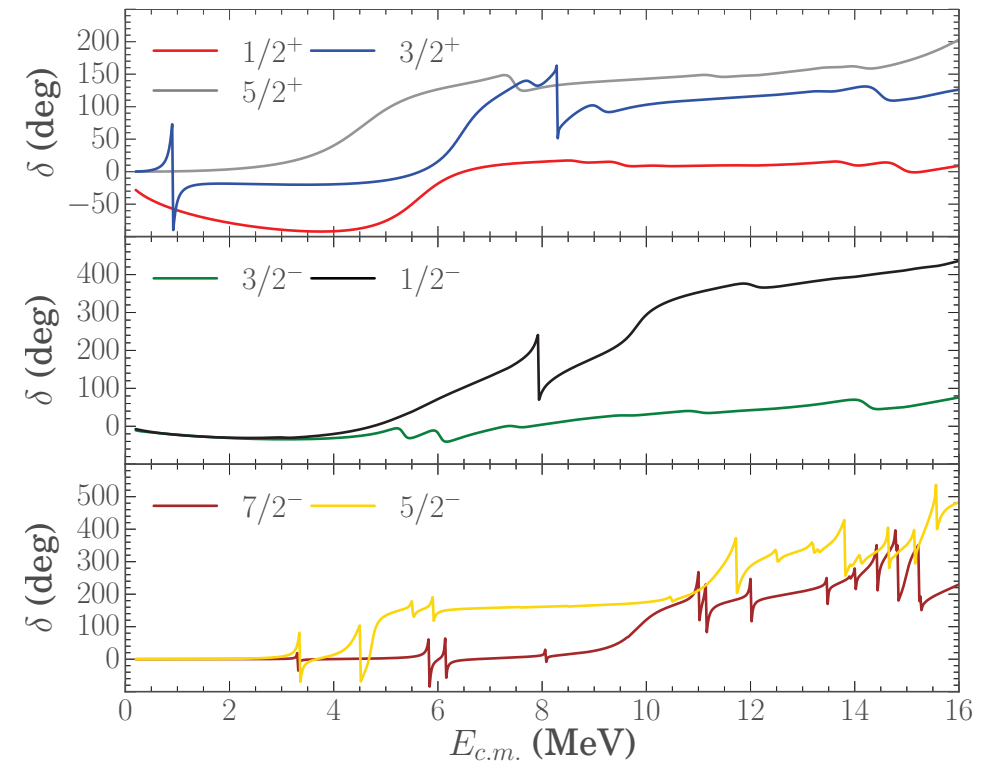


TABLE I. Excitation spectrum of ^{17}O with respect to the $n+^{16}\text{O}$ threshold, as obtained from Eq. (5) and the NNLO_{sat} interaction and compared to the experiment [45]. Broad resonances in the continuum (most notably, the $5/2^+$) are computed at midpoint. The asterisks (*) indicate higher excited states, above the lowest one, for each partial wave.

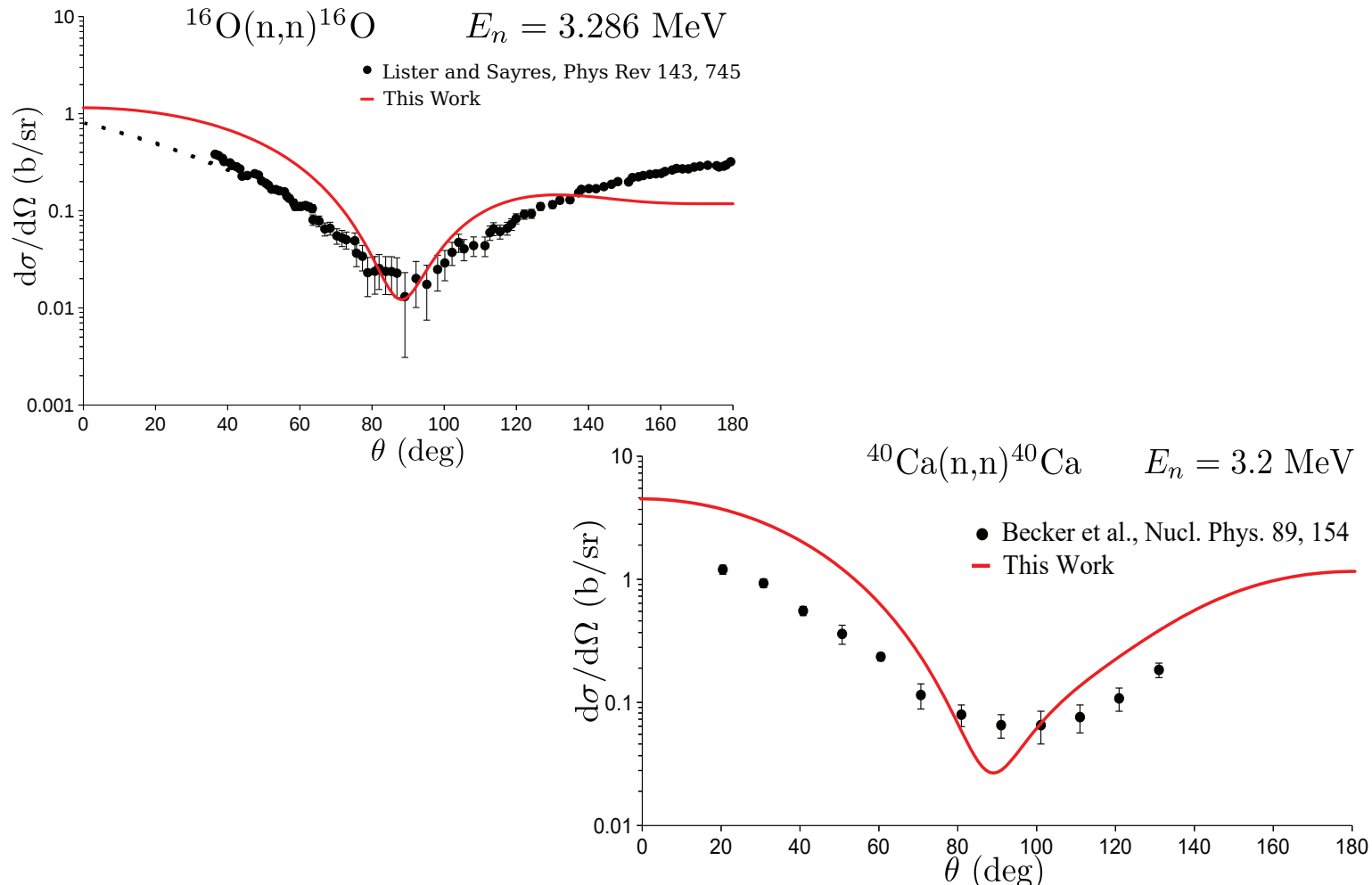
Full self-energy from SCGF:



O

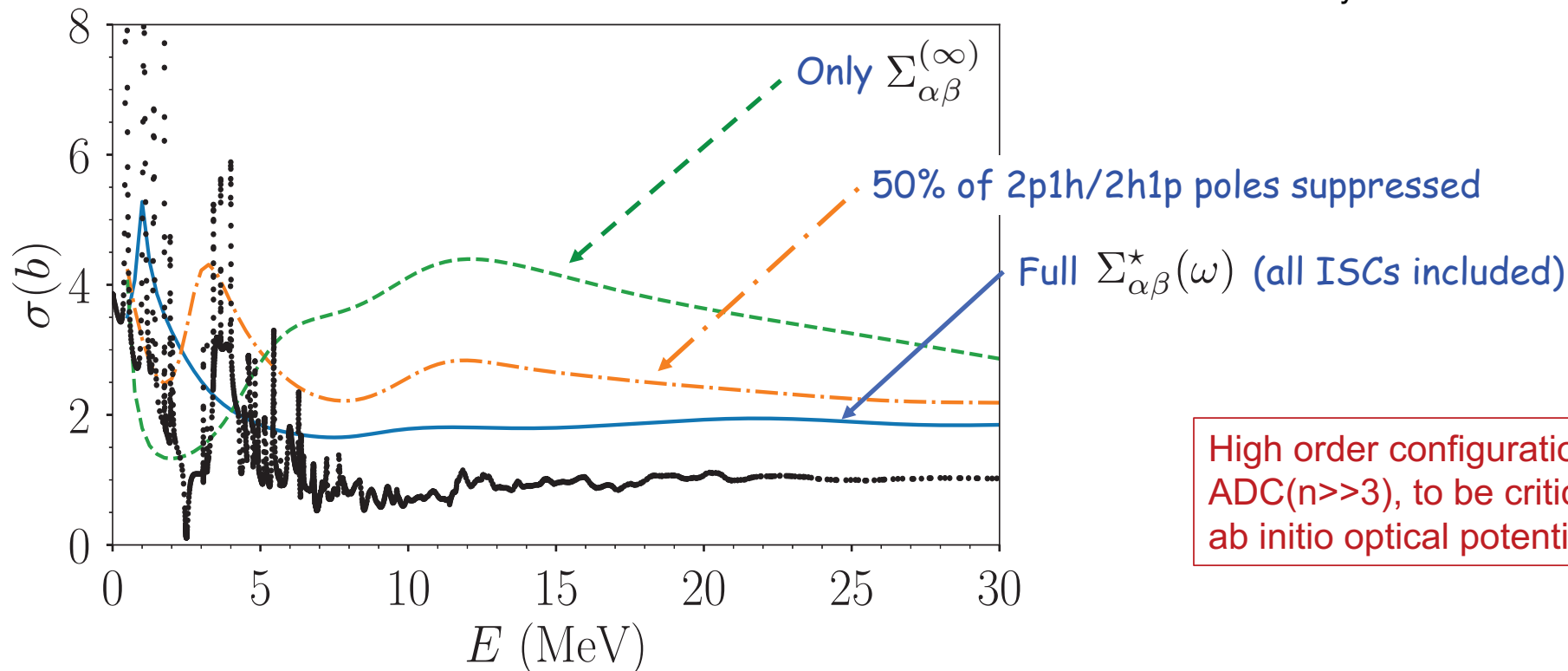
Low energy scattering - from SCGF

[A. Idini, CB, Navrátil, PRL123, 092501 (2019)]



Role of intermediate state configurations (ISCs)

$n-^{16}O$, total elastic cross section



[A. Idini, CB, Navratil,
Phys. Rev. Lett. **123**, 092501 (2019)]

High order configurations, or
ADC($n > 3$), to be critical for fully
ab initio optical potentials

$$\Sigma_{\alpha\beta}^*(\omega) = \Sigma_{\alpha\beta}^{(\infty)} + \sum_{i,j} \mathbf{M}_{\alpha,i}^\dagger \left[\frac{1}{E - (\mathbf{K}^> + \mathbf{C}) + i\Gamma} \right]_{i,j} \mathbf{M}_{j,\beta} + \sum_{r,s} \mathbf{N}_{\alpha,r} \left[\frac{1}{E - (\mathbf{K}^< + \mathbf{D}) - i\Gamma} \right]_{r,s} \mathbf{N}_{s,\beta}^\dagger$$

2p1h 2h1p

Reaching large isotopes

(electron scattering and charge radii)

CB, P. Arthuis – Preliminary... (work in progress)

Electron-Ion Trap colliders...

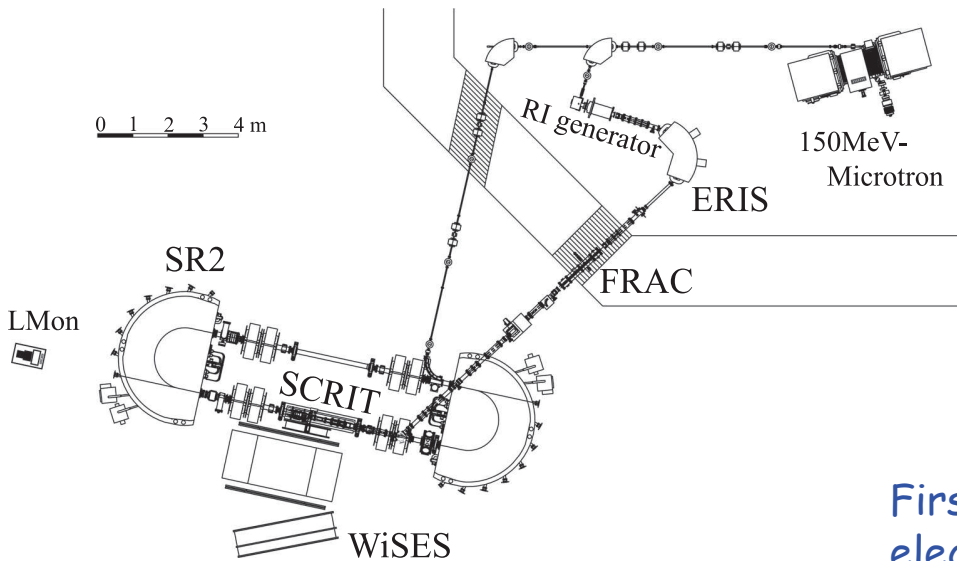


FIG. 1. Overview of the SCRIT electron scattering facility.

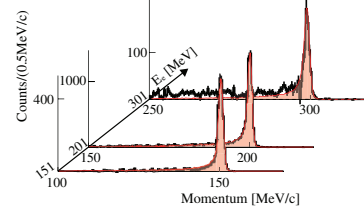
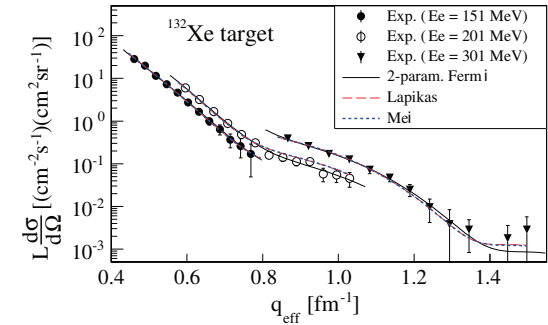


FIG. 3. Reconstructed momentum spectra of ^{132}Xe target after background subtraction. Red shaded lines are the simulated radiation tails following the elastic peaks.

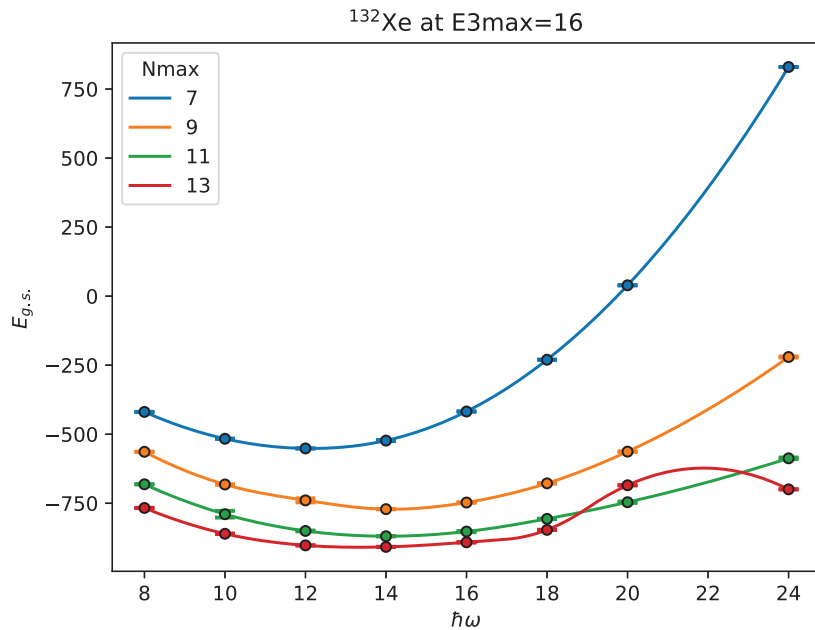


First ever measurement of charge radii through electron scattering with and ion trap setting that can be used on radioactive isotopes !!

K. Tsukada *et al.*, Phy rev Lett **118**, 262501 (2017)

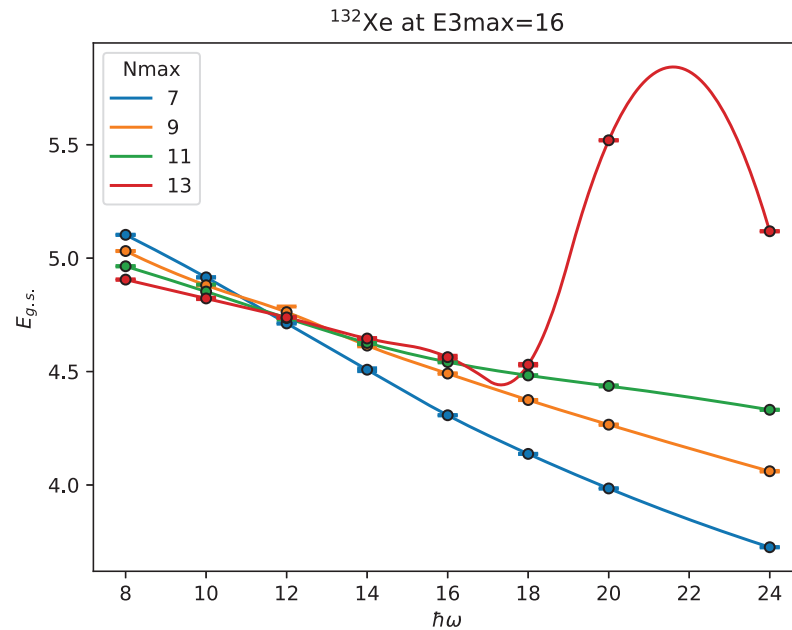
Convergence in large isotopes - e.g. ^{132}Xe

Gorkov ADC(2) with NNLOsat Hamiltonian



Energies still badly converging...

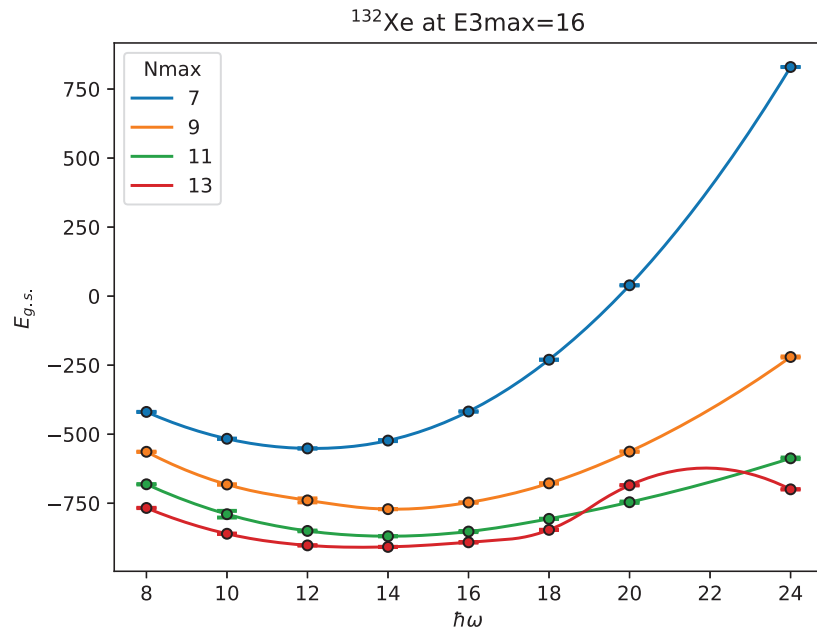
- Nmax converges slowly...
- E3max (# of 3NFs elements) out of control



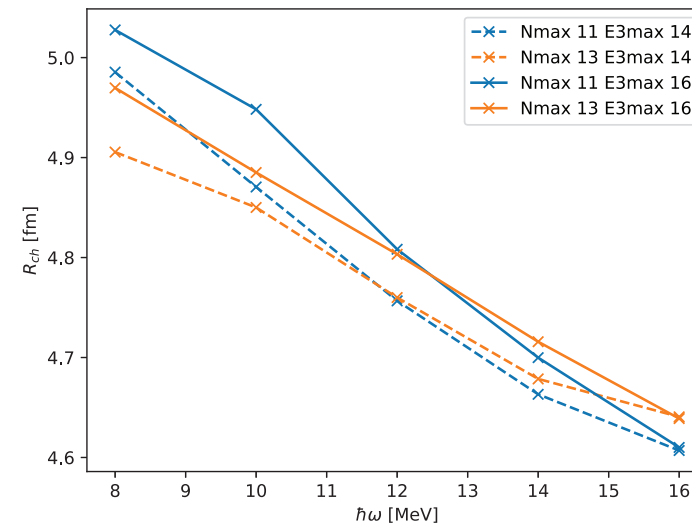
Radii converge much better and can be bracketed!

Convergence in large isotopes - e.g. ^{132}Xe

Gorkov ADC(2) with NNLOsat Hamiltonian



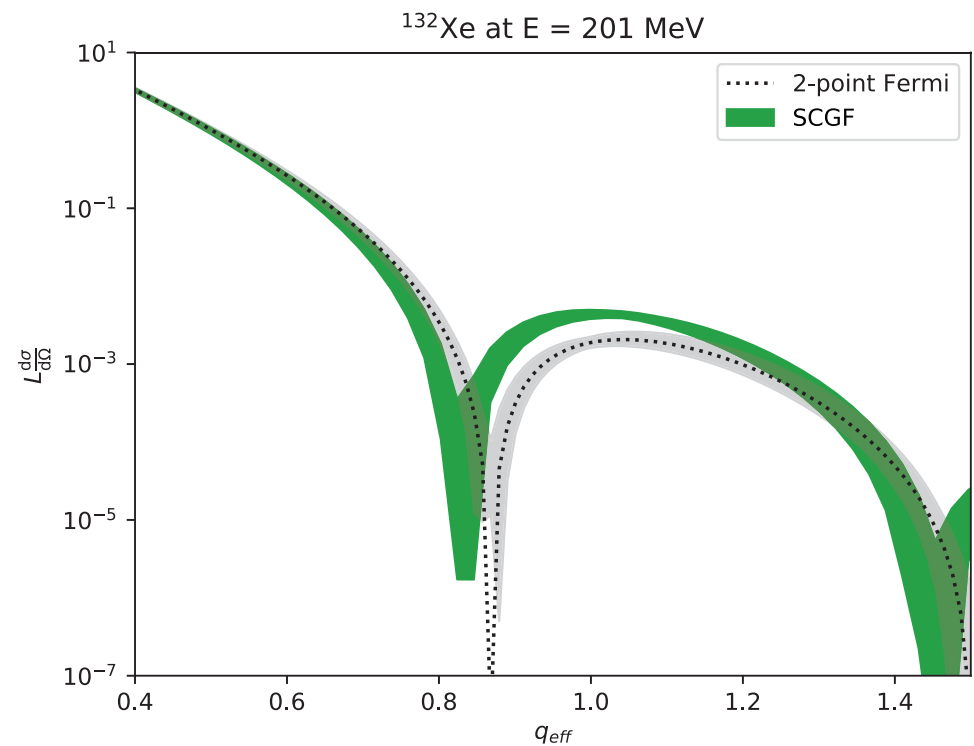
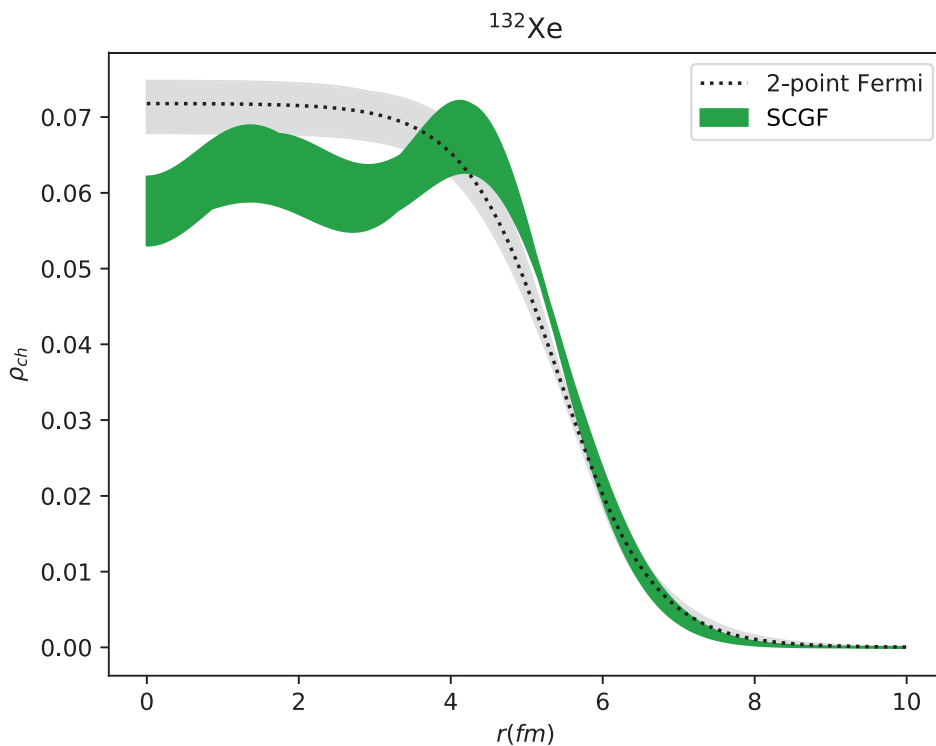
Energies still badly converging...
- Nmax converges slowly...
- E3max (# of 3NFs elements) out of control



Radii converge much better and
can be bracketed!

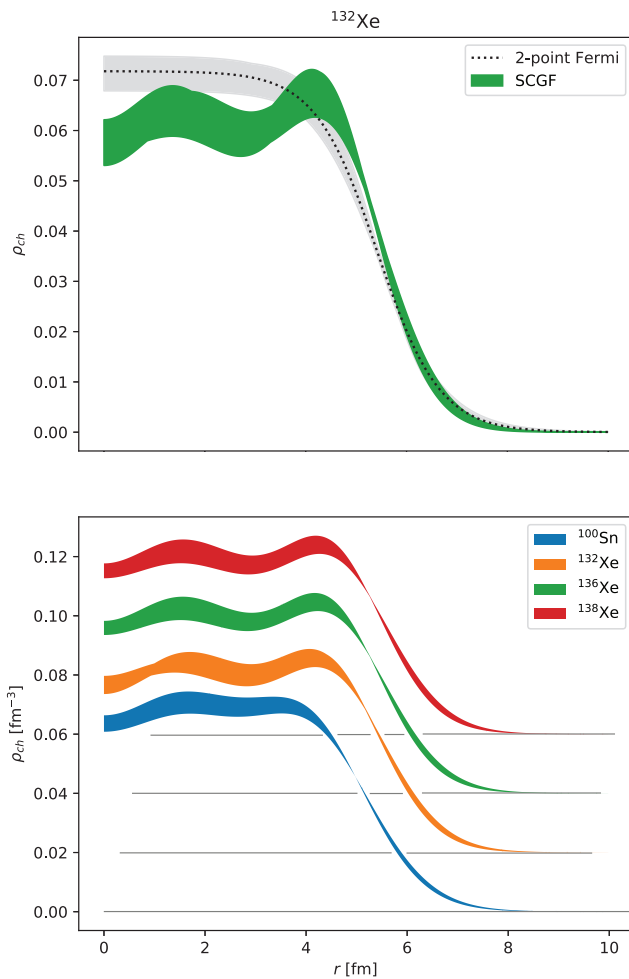
Convergence in large isotopes - e.g. ^{132}Xe

Gorkov ADC(2) with NNLOsat Hamiltonian



Sn and Xe isotopes

Gorkov ADC(2) and Dyson ADC(3) with NNLOsat Hamiltonian



	SCGF	Exp.
^{100}Sn	4.525 – 4.707	
^{132}Sn	4.725 – 4.956	4.7093
^{132}Xe	4.700 – 4.948	4.7859
^{136}Xe	4.715 – 4.928	4.7964
^{138}Xe	4.724 – 4.941	4.8279

Preliminary !!

Electron and neutrino scattering off nuclei

N. Rocco, CB, Phys. Rev. C98, 025501 (2018)

N. Rocco, CB, O. Benhar, A. De Pace, A. Lovato, Phys. Rev. C99, 025502 (2019)

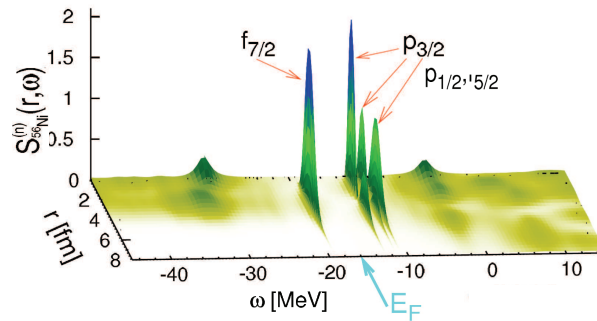
CB, N. Rocco, V. Somà, arXiv:1907.01122

Lepton-nucleon cross section

$$\left(\frac{d\sigma}{dT' d\cos\theta'} \right)_{\nu/\bar{\nu}} = \frac{G^2}{2\pi} \frac{k'}{2E_\nu} \left[\hat{L}_{CC} R_{CC} + 2\hat{L}_{CL} R_{CL} + \hat{L}_{LL} R_{LL} + \hat{L}_T R_T \pm 2\hat{L}_{T'} R_{T'} \right],$$

Nuclear structure is in the hadronic tensor:

$$W^{\mu\nu}(\mathbf{q}, \omega) = \int \frac{d^3k}{(2\pi)^3} dE P_h(\mathbf{k}, E) \frac{m^2}{e(\mathbf{k})e(\mathbf{k} + \mathbf{q})} \times \sum_i \langle k | j_i^{\mu\dagger} | k + q \rangle \langle k + q | j_i^\nu | k \rangle \times \delta(\omega + E - e(\mathbf{k} + \mathbf{q})),$$



$$R_{CC} = W^{00}$$

$$R_{CL} = -\frac{1}{2}(W^{03} + W^{30})$$

$$R_{LL} = W^{33}$$

$$R_T = W^{11} + W^{22}$$

$$R_{T'} = -\frac{i}{2}(W^{12} - W^{21}),$$

$$W^{\mu\nu} = \sum_f \langle 0 | j^{\mu\dagger} | f \rangle \langle f | j^\nu | 0 \rangle \delta(E_0 + \omega - E_f)$$

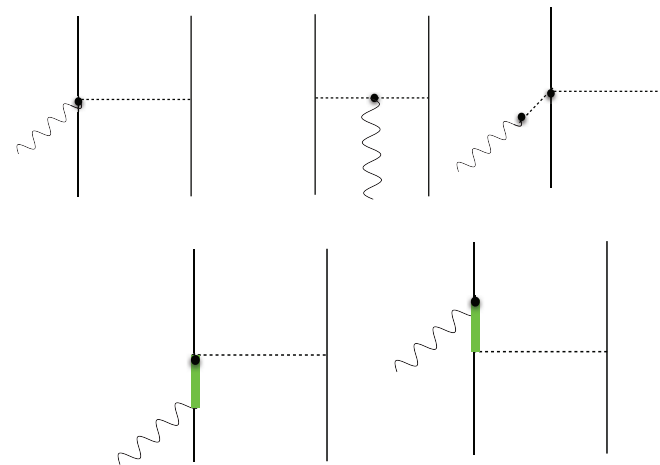
Lepton-nucleon cross section

$$\left(\frac{d\sigma}{dT' d \cos \theta'} \right)_{\nu/\bar{\nu}} = \frac{G^2}{2\pi} \frac{k'}{2E_\nu} \left[\hat{L}_{CC} R_{CC} + 2\hat{L}_{CL} R_{CL} + \hat{L}_{LL} R_{LL} + \hat{L}_T R_T \pm 2\hat{L}_{T'} R_{T'} \right],$$

Nuclear structure is in the hadronic tensor:

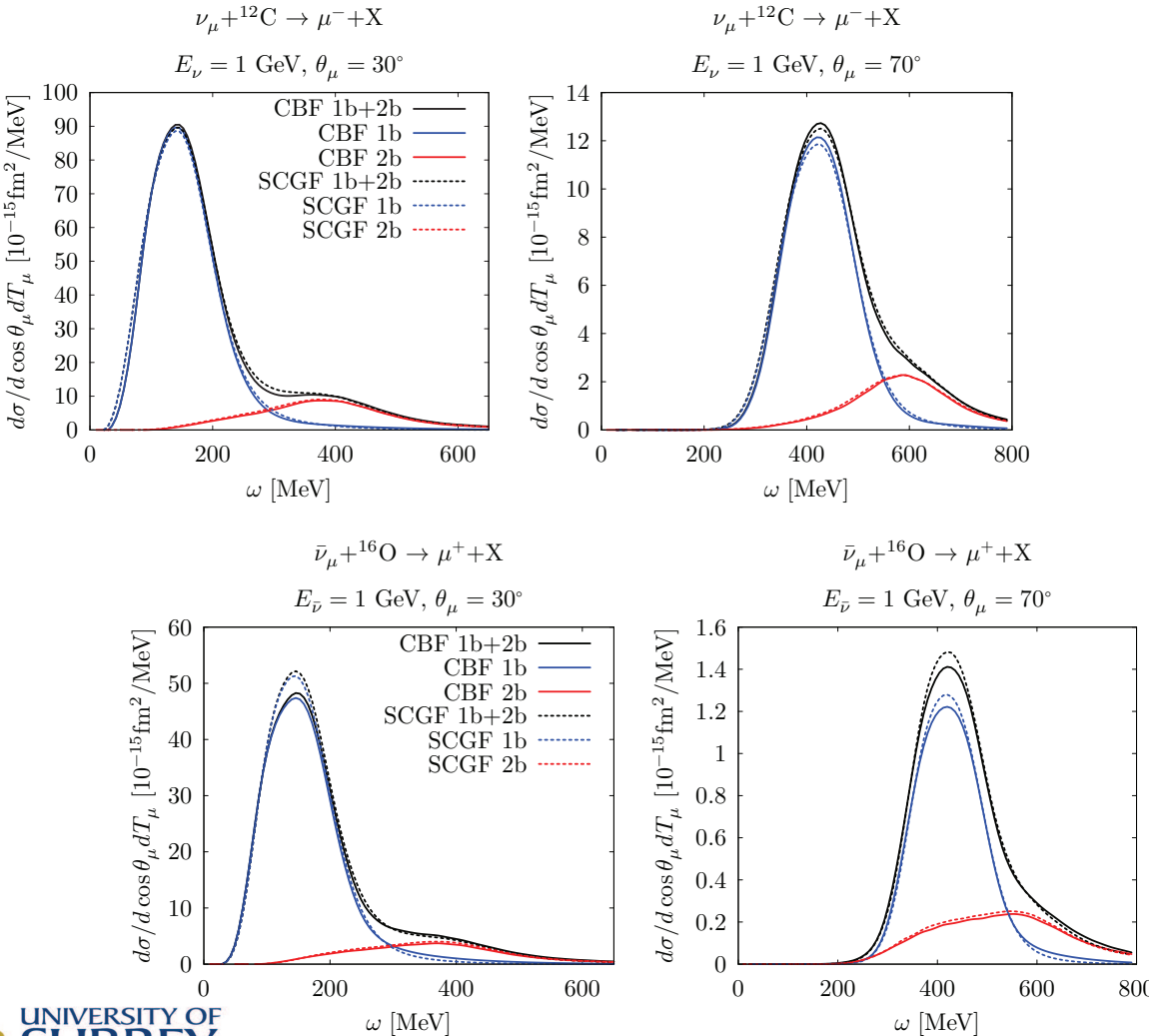
$$W^{\mu\nu}(\mathbf{q}, \omega) = \int \frac{d^3 k}{(2\pi)^3} dE P_h(\mathbf{k}, E) \frac{m^2}{e(\mathbf{k}) e(\mathbf{k} + \mathbf{q})} \\ \times \sum_i \langle k | j_i^{\mu\dagger} | k + q \rangle \langle k + q | j_i^\nu | k \rangle \\ \times \delta(\omega + E - e(\mathbf{k} + \mathbf{q})),$$

Two-body diagrams contributing to the axial and vector responses



$$W_{2b}^{\mu\nu}(\mathbf{q}, \omega) = \frac{V}{2} \int d\tilde{E} \frac{d^3 k}{(2\pi)^3} d\tilde{E}' \frac{d^3 k'}{(2\pi)^3} \frac{d^3 p}{(2\pi)^3} \\ \times \frac{m^4}{e(\mathbf{k}) e(\mathbf{k}') e(\mathbf{p}) e(\mathbf{p}')} P_h^{NM}(\mathbf{k}, \tilde{E}) P_h^{NM}(\mathbf{k}', \tilde{E}') \\ \times \sum_{ij} \langle k' | j_{ij}^{\mu\dagger} | pp' \rangle \langle pp' | j_{ij}^\nu | k' \rangle \\ \times \delta(\omega + \tilde{E} + \tilde{E}' - e(\mathbf{p}) - e(\mathbf{p}')). \quad (41)$$

Charged-current reaction for 1 GeV neutrinos



One-body current describe quasi elastic peak

Difference between CBF(AV18) and SCGF(NNLOsat) from 1-b terms

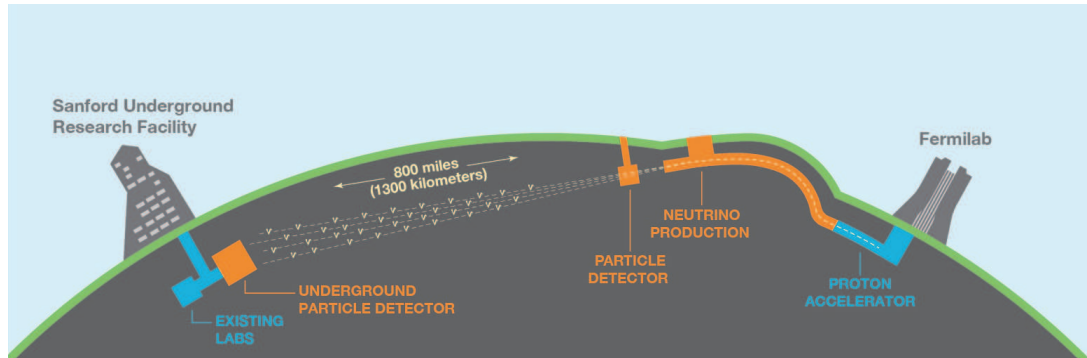
Two-body currents full up dip region

Missing Delta and meson emission contributions

X-sec. dropping with scattering angle

N. Rocco, CB, O. Benhar, de Pace , A. Lovato, Phys. Rev. C99, 025502 (2019)

Neutrino Oscillations - next generation experiments



DUNE experiment will measure long base line neutrino oscillations to:

- Resolve neutrino mass hierarchy
- Search for CP violation in weak interaction
- Search for other physics beyond SM



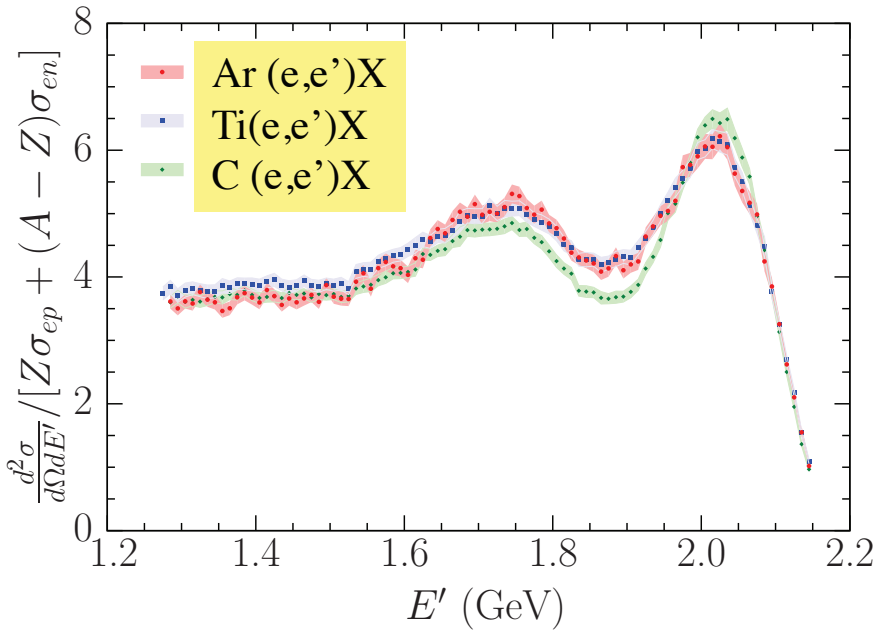
Liquid Argon projection chamber is being used. It will require one order of magnitude ($20\% \rightarrow 2\%$) improvement in theoretical prediction for $\nu\text{-}{}^{40}\text{Ar}$ cross sections to achieve proper event reconstruction.

→ Need good knowledge of ${}^{40}\text{Ar}$ spectral functions and consistent structure-scattering theories.

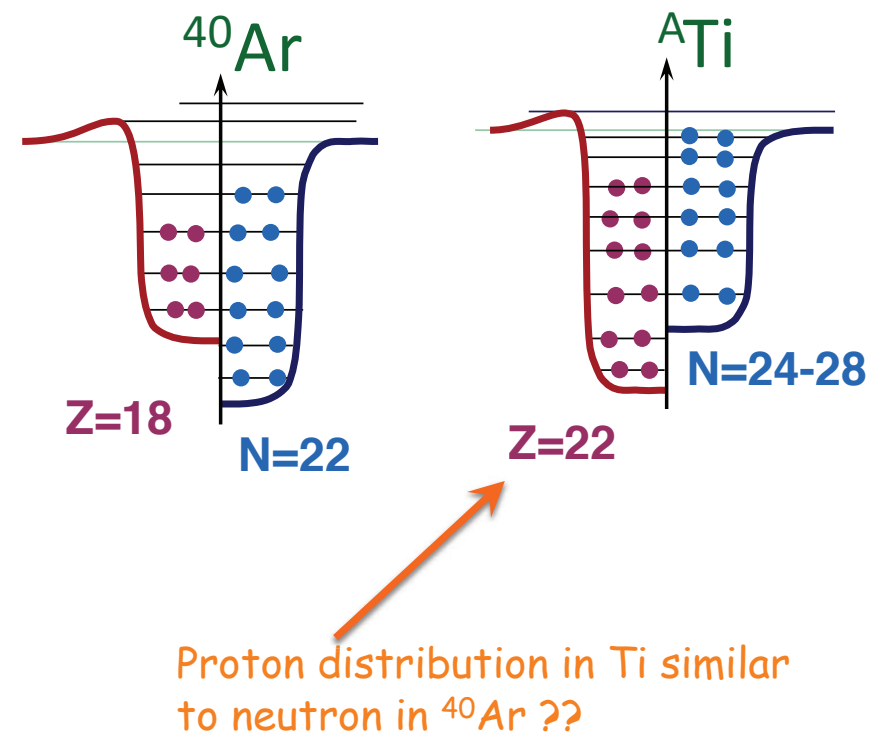
Spectral function for ^{40}Ar and Ti

Jlab experiment E12-14-012 (Hall A)

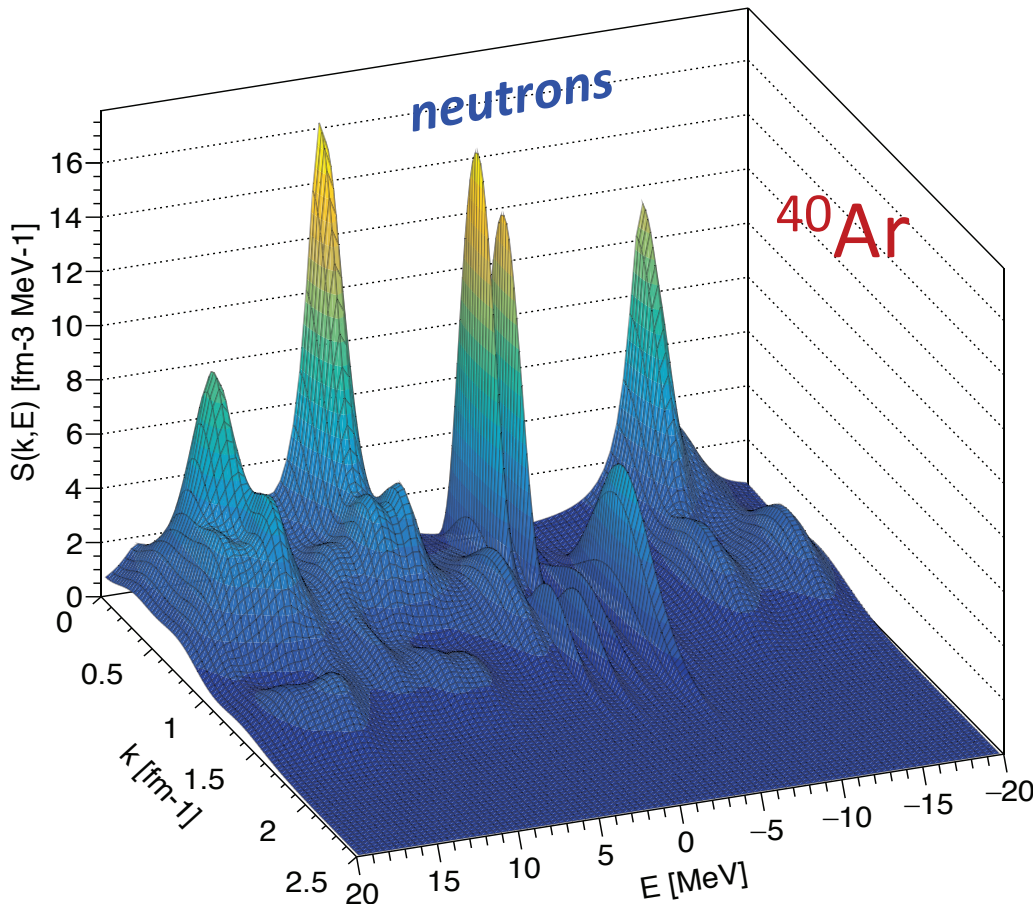
Phys. Rev. C 98, 014617 (2018); arXiv:1810.10575



$^{40}\text{Ar}(e,e'p)$ and $\text{Ti}(e,e'p)$ data being analyzed



Spectral function for ^{40}Ar



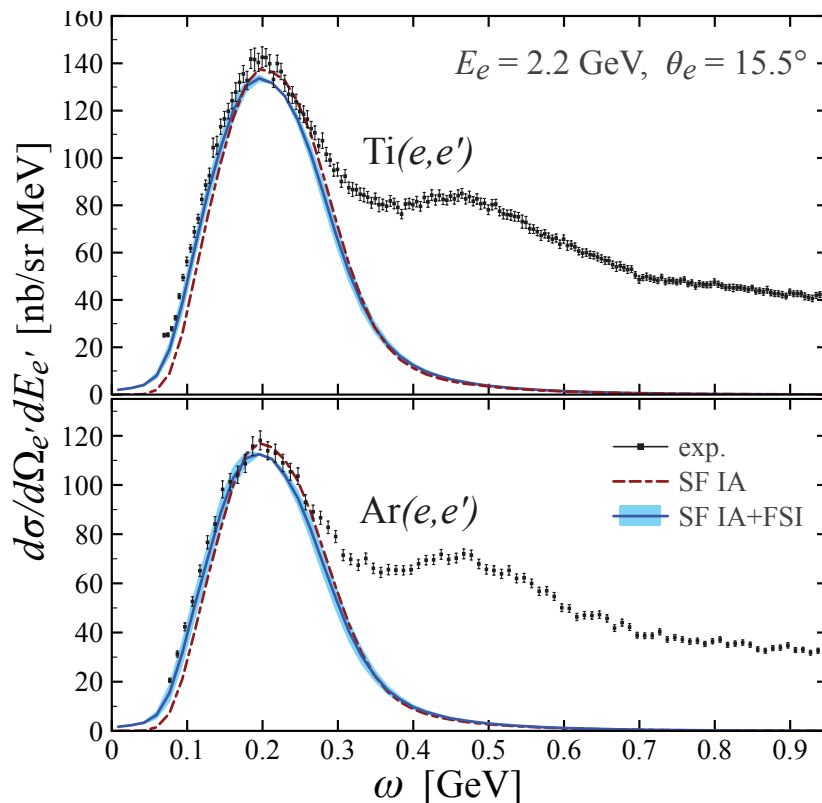
- Experimental data now available from Jlab:
H. Dai et al., arXiv:1803.01910/ 1810.10575
 - Ab initio simulations based on the ADC(2) truncation of the N2LO-sat Hamiltonian
- Want validation of initial state correlation
before they are implemented in neutrino- ^{40}Ar simulations

CB, N. Rocco, V. Somà, arXiv:1907.01122

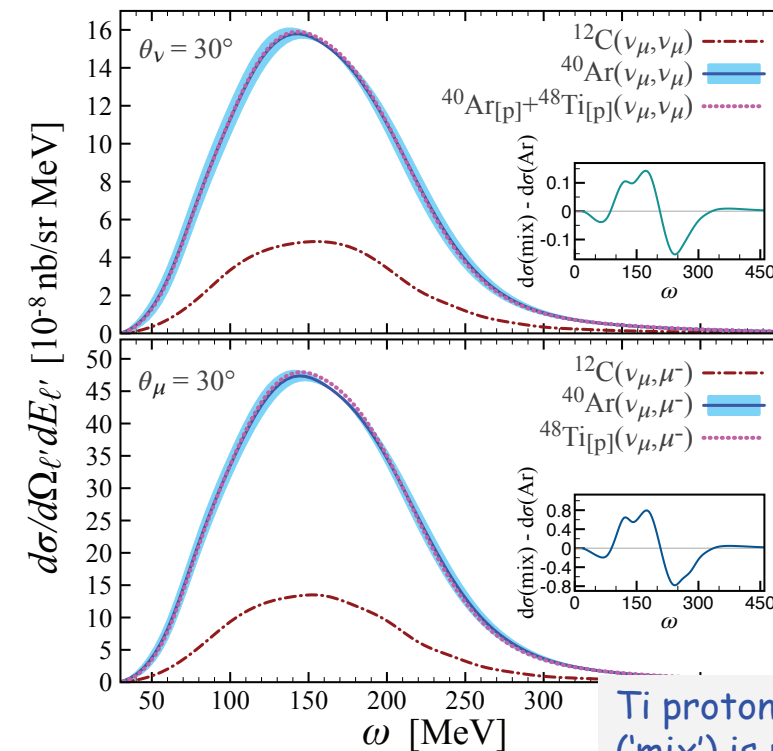
Electron and ν scattering on ^{40}Ar and Ti

Jlab experiment E12-14-012 (Hall A)

[Phys. Rev. C 98, 014617 (2018)]



$^{40}\text{Ar}(e,e'p)$ and $\text{Ti}(e,e'p)$ data being analyzed



Ti protons contribution ('mix') is nearly identical to neutrons in ^{40}Ar .

Collaborators

Thank you for your attention!!!



A. Cipollone

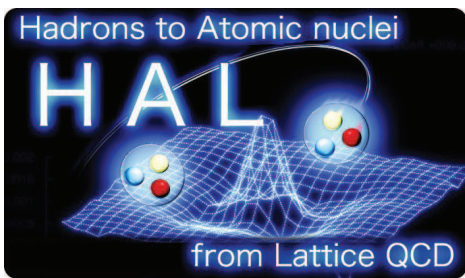
A. Rios, A. Idini, P. Arthuis, M. Drissi



V. Somà, T. Duguet, F. Raimondi



D. Lonardoni, S. Gandolfi



S. Aoki,

T. Doi, T. Hatsuda,

T. Inoue,

H. Nemura

YITP Kyoto Univ.

RIKEN Nishina

Nihon Univ.

Univ. Tsukuba



A. Carbone



P. Navratil



A. Lovato, N. Rocco

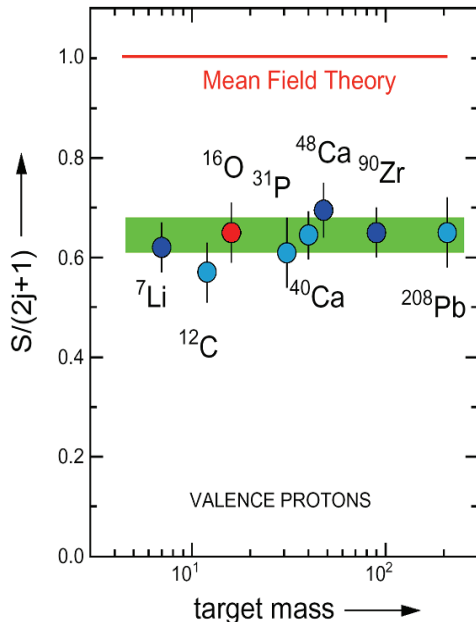


Backup Slides

Spectroscopic factors

Quenching of SF in stable nuclei

NIKHEF:
Nucl. Phys. A553 (1993) 297c



- Short-range correlations oriented methods:
 - VMC [Argonne, '94] 0.90
 - GF(SRC) [St.Louis-Tübingen '95] 0.91 0.89
 - FHNC/SOC [Pisa '00] 0.90
- Including particle-phonon couplings:
 - GF(FRPA) [St.Louis '01] 0.77 0.72
[CB et al., Phys. Rev. C65, (02)]
- Experiment ($e, e'p$): 0.63 0.67 ± 0.07
(estimated uncertainty)

SRC are present and verified experimentally

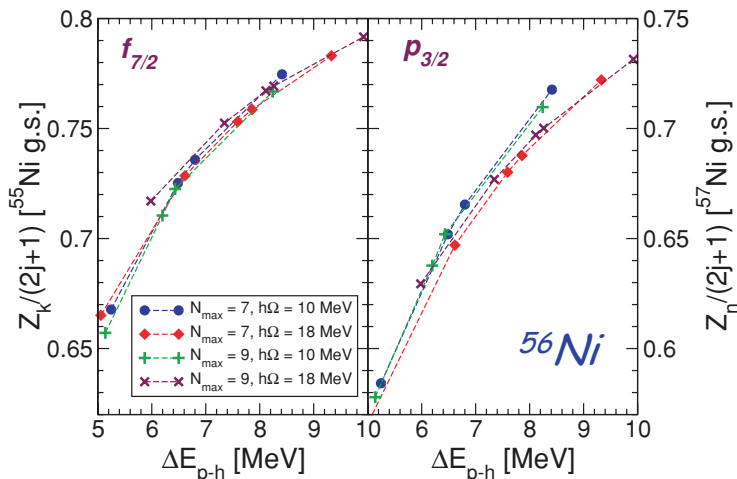
BUT they are NOT the dominant mechanism for quenching SF!!!

Z/N asymmetry dependence of SFs - Theory

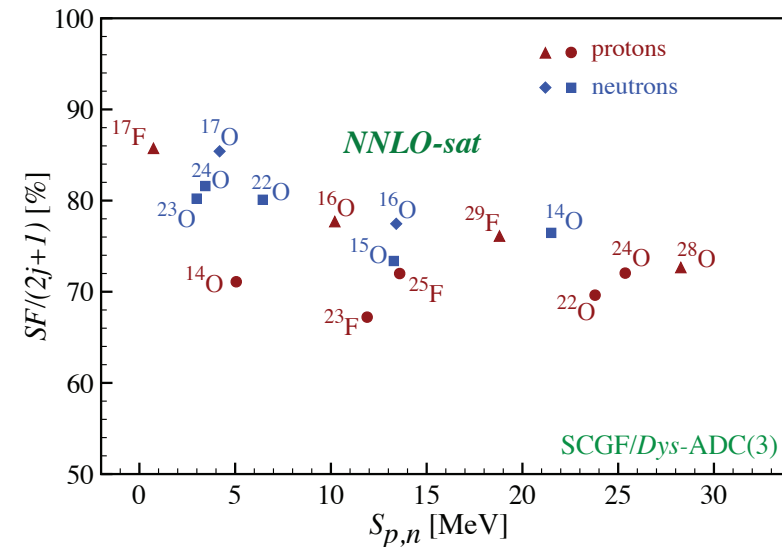
Ab-initio calculations explain (a very weak) the Z/N dependence but the effect is much lower than suggested by direct knockout

Rather the quenching is high correlated to the gap at the Fermi surface.

Spectroscopic factor are strongly correlated to p-h gaps:



CB, M. Hjorth-Jensen,
Phys. Rev. C **79**, 064313 (2009)



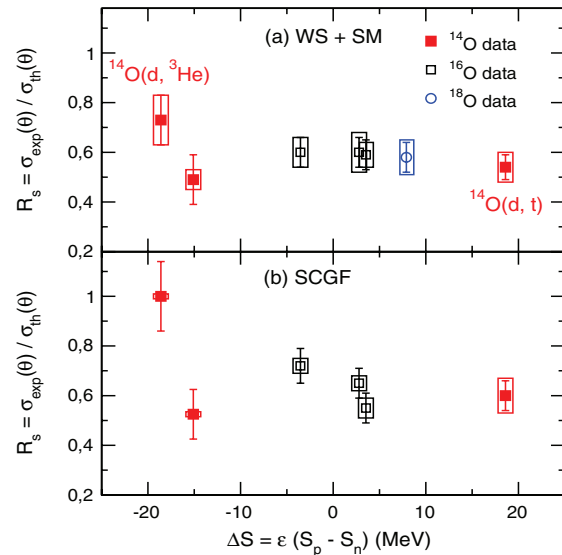
A. Cipollone, CB, P Navrátíl, Phys. Rev. C **92**, 014306 (2015)
and CB, unpublished (2016)

Z/N asymmetry dependence of SFs

Calculated spectroscopic factors are found to be:

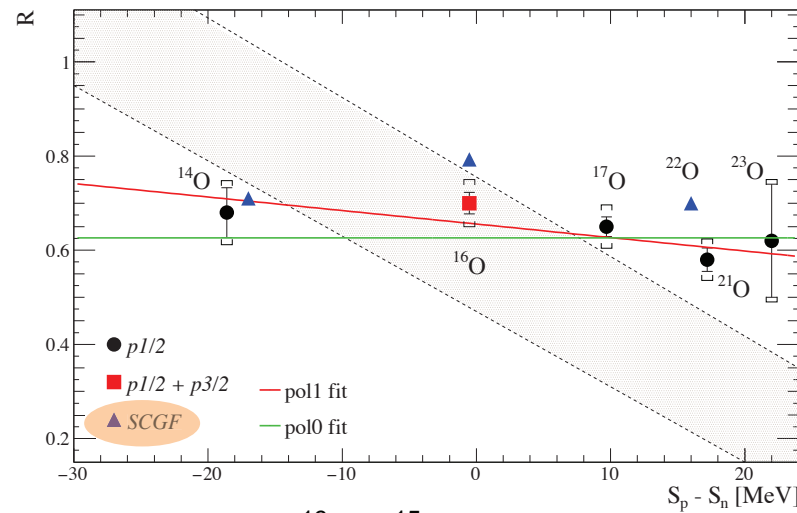
- correlated to p-h gaps
- independent of asymmetry
- consistent with experimental data

$^{14}\text{O}(\text{d},\text{t})^{13}\text{O}$ and $^{14}\text{O}(\text{d},{}^3\text{He})^{13}\text{N}$
transfer reactions @ SPIRAL



[F. Flavigny et al, PRL110, 122503 (2013)]

$^A\text{O}(\text{p},2\text{p})^{A-1}\text{N}$ at GSI ($\text{R}^3\text{B-LAND}$)



Proton SF for $^{16}\text{O} \rightarrow ^{15}\text{N}$:

- | | | |
|-------------|--------------------|----------------------------------|
| $p_{1/2}$: | 0.78 (SCGF) | 0.80 (exp.) |
| $p_{3/2}$: | 0.80 (SCGF) | 0.65 (exp. – up to cont.) |

L. Atar, et al., Phys. Rev. Lett 120, 52501 (2018)